8/3/2001 3:44:37 PM

Autonomous Sciencecraft Constellation Science Study Report
New Millennium Program Space Technology 6 (NMP-ST6)
Techsat-21 Mission

Science Team

Ashley G. Davies
Jet Propulsion Laboratory-California Institute of Technology, Pasadena, CA.

Ronald Greeley and Kevin Williams
Department of Geological Sciences, Arizona State University, Tempe, AZ.

Victor Baker and James Dohm
Hydrology and Water Resources, University of Arizona, Tucson, AZ.

Onboard Science Team

Mike Burl, Eric Mjolsness, Rebecca Castano, Tim Stough, Joseph Roden
Jet Propulsion Laboratory-California Institute of Technology, Pasadena, CA.

ASC P.I. Steve Chien
Jet Propulsion Laboratory-California Institute of Technology

Project Manager: Robert Sherwood
Jet Propulsion Laboratory-California Institute of Technology, Pasadena, CA.

Contents

Figures

Tables

Executive Summary

Many physical processes have combined to first form and then alter the surface of Earth, and many of these processes have analogs that mold the surfaces of other planetary bodies. The Autonomous Sciencecraft Constellation (ASC) is a science experiment that will fly on the Air Force Research Laboratory Techsat-21 (Technology Satellite for the 21st Century) spacecraft in July 2004. The science goal of the ASC mission is to demonstrate autonomous control over data collection and autonomously carry out scientific analysis of large datasets (in this case, radar images), returning both those data with the highest scientific value as well as selected scientific analyses of the data, thus negating the need to return the entire dataset. Data where no change is detected from previous observations is discarded: only a "no change" flag is set. ASC will demonstrate the use of change detection and feature identification software to autonomously process data on-board the spacecraft. This allows the best use of very limited downlink to return the most scientifically valuable data and products first, as well as the rapid and autonomous reaction to new events of high scientific interest through resources allocated by an onboard planner.

Although this mission uses radar, we stress that the data processing *techniques* can be applied to data obtained from any instrument collecting data from anywhere in the electromagnetic spectrum. The Techsat-21 ASC mission consists of a three-satellite constellation in Earth orbit. Each satellite is equipped with X-band synthetic aperture radar (SAR). Successful demonstration of this technology will open new avenues for exploring the Solar System, realizing the attainment of a major milestone on NASA's road to exploring the Solar System. A system that can selectively return the most valuable data from huge datasets eases congestion on the Deep Space Communications Network (DSN) while maximizing the science content of each byte of data returned. To achieve this, ASC utilizes onboard data processing techniques to both detect change on the surface of the Earth and to recognize specific features. These capabilities will be used to detect and monitor several geomorphological processes on Earth, all of which have extraterrestrial analogs, such as the formation and retreat of ice, and the emplacement of lava flows and other volcanic deposits. The ability to rapidly replan observations and allocate resources in response to onboard processing of data is a step beyond current capabilities. Using these techniques, rare transient events (such as "outburst" eruptions on Io, to use an extraterrestrial example) can be instantly allocated observation time once detected.

The image processing and scientific analysis techniques described in this study report are not confined to radar data of Earth. The techniques have widespread applications, theoretically to any instrument at any wavelength (such as visible and infrared imagers). We illustrate how the same techniques demonstrated by ASC can be used to search for change, and identify features, on Mars and the jovian satellites, Europa and Io.

ASC will initially fly in Earth orbit for one year (July 2004-July 2005) during which a number of command and control, calibration, science and reconfiguration experiments will be carried out. An Extended ASC mission for a further year with a greater proportion of the time dedicated to the science mission. It is anticipated that as much as 1 terabyte of science data could be returned during a two-year mission.

26 October 2021, 956 million kilometers from Earth.
Io Orbit Insertion

The Volcan *spacecraft fires its main engine and in the final stage of a long, difficult journey enters a highly elliptical orbit around the Jovian satellite, Io. The high radiation environment means that the operational lifetime of the spacecraft is short: not a second must be wasted. The driving mission objective is to unlock the mysteries of Io, the most dynamic satellite in the Solar System. This mission will determine if the transfer of Jupiter's orbital energy, through Io to Europa via an orbital resonance, is sufficient to generate silicate volcanism, deep below the Icy Europan crust. Where there is volcanism and water, life may evolve.* Volcan's *other main objective is to monitor volcanic activity on Io, at high temporal, spatial and spectral resolution. Onboard, the computer consults the lists of prioritized targets, while instruments scan the surface of the satellite, identifying areas of new lava flow emplacement and new plume deposits (some over 1000 km across) and identifying long-lived volcanoes that have been active for decades. A laser altimeter creates profiles of the surface: the orbital trajectory yields clues to internal structure and heating mechanisms. Visual, infrared and ultraviolet data are compared with on-board databases of every Io observation obtained over half a century to evaluate the changes observed. Suddenly, the IR camera registers a thermal pulse so intense it momentarily blinds the sensor. Re-calibrating, the camera fits the short and long IR spectra with models of volcanic thermal emission and concludes that a massive volcanic eruption is starting: fifty-thousand kilometers away, high temperature lava has forced its way to the surface of Io. Powered by rapidly exsolving gases, the lava is erupting at a rate of thousands of tonnes every second, forming a fountain of incandescent lava 10 kilometers high and massive, fast-moving flows on the surface. Sulphur-rich ices boil into space: red and blue aurora flicker. Such an outburst is a rare, short-lived event: it may not happen again during the lifetime of* Volcan. *There is no time to consult Earth: round-trip communication time is nearly two hours, and the trajectory of the spacecraft will take it beyond view of this eruption in minutes. Besides, Io is in eclipse behind Jupiter so communication with Earth is impossible. After consulting the existing list of prioritized targets, the onboard planner immediately retargets the other instruments to observe the phenomenon. Hundreds of observations are made and gigabytes of data are collected. With a puff of propellant a disposable probe is dropped onto the feature: it will transmit images and spectral analyses until destroyed. On* Volcan *the computer software compiles the data, extracts temperature/area distributions and vital compositional data, rates of eruption rates, gas species and volatile content, marks the analyses as "high priority" and adds the data products to the downlink array. Already, early in the mission, an important process has been observed and an objective met! The mission objective is assigned a lower priority by the onboard planner.* Volcan *continues running through its self-generated observation sequences. The data are continuously scanned for the distinctive shapes of impact craters and volcanic plumes. And now data from the probe are arriving: the planner allocates processing time to this high-priority dataset as processors continue evaluating the other data streaming in...*

1.0 Introduction

Autonomous instrument and spacecraft control, and autonomous processing and understanding of data, will add flexibility to future missions where high-science value events may be transitory. For example, the Galileo spacecraft is in orbit around Jupiter and regularly observing volcanism on Io. The selection of targets is made months ahead of each orbital encounter and a pre-determined sequence of commands is uploaded to the spacecraft. However, volcanism on Io (see section 2.3) is an extremely dynamic system, and often events proceed faster than the ability to change observation sequences. The use of autonomous analysis of data in real time in Jupiter orbit allows the most fleeting events to be observed at very short notice, these events (such as the Io thermal "outbursts" being both rare, and of short-duration.

As scientific instruments on spacecraft become more sophisticated and data collection becomes more efficient, the volumes of data collected during the lifetime of a mission may run into terabytes. A multinational Mars exploration program is underway, with more than a dozen spacecraft planned to orbit or land on Mars in the next decade. Varied instrumentation on these spacecraft will generate vast datasets that could become unmanageable. In addition, as more and more missions spread out into the Solar System and beyond, other potential problems arise. These include a communications bottleneck as missions vie for downlink and uplink time, placing a strain on deep-space communications, and extensive communication time-lags which translate into tremendous mission expense. These and other potential problems using traditional onboard software make it unfeasible to explore remotely large expanses of planetary surfaces. In order to make future missions more communication efficient and cost and science effective, such as in situations where decisions/observations/actions need to be made in situ, missions with traditional technologies will have to be replaced with autonomous sciencecraft.

Traditionally, spacecraft have been controlled through linear (non-branching) command sequences that have been painstakingly designed on the ground. Recently NASA has been making technological advances towards enabling autonomous spacecraft, using onboard science, planning, and execution agents. Spacecraft capable of such onboard, science-directed autonomy will revolutionize space missions by enabling: (1) onboard estimation of the science value of data to prioritize data (such as by change detection or deviation from predicted models) and to direct future observations, (2) faster recovery from spacecraft anomalies, increasing science time and resources, and (3) the design of spacecraft operations that will maximize the value of science observations by utilizing actual execution feedback rather than conservative open-loop estimates (as often required by ground-based sequencing).

The main science objectives of the Autonomous Sciencecraft Constellation (ASC) mission are to demonstrate that process-related change and feature identification can be made during space flight. This mission will study geological and environmental processes on Earth using X-band SAR. Examples of geologic processes that may be observed/investigated include (but are not limited to) active volcanism, the movement of sand dunes and transient features in desert environments, the ebb and flow of ice formation on lakes and mountains, and storm-induced flooding of devastating proportions. This effort will have a direct bearing on future science-driven missions to other planetary bodies, because such geologic activity is observed elsewhere in the solar system. ASC will demonstrate the revolutionary concept of onboard processing to analyze science data in order to determine spacecraft activities. This onboard processing will consist of several components: *onboard science*, *onboard replanning*, and *cluster management*.

Science software placed on board the sciencecraft will allow autonomous processing and formation of Synthetic Aperture Radar (SAR) images and extraction of scientific information in situ, including feature identification and change, resulting in minimization of excess data, a maximization of useful scientific return, and a significant savings of time and cost. In addition, this technology will allow us to use more efficiently valuable downlink bandwidth to observe geologic phenomena such as flooding, melting of ice, and the emplacement of lava flows here on Earth and elsewhere in the solar system and beyond (more effective use of valuable downlink bandwidth). Science-driven goals will evolve during the ASC mission through onboard replanning software that will generate low-level command sequences based on reformulation of science goals from the onboard science software. Finally, *Cluster management* software will enable the elements of the distributed spacecraft constellation to work as a single virtual instrument.

Together, these State-of-the-Art software packages will yield increased science return per downlink as well as overall mission science return. The ability to respond onboard to the results of science observations will enable a whole new class of missions in which scientists will receive the most relevant scientific data, including capturing short-lived phenomena such as transient volcanic eruptions and the identification of new impact crater sites on planets and moons. Change-based triggering and model-based event detection will also enable reasonable data volumes for extended duration missions to detect and monitor surface change on, for example, Mars, Io, Triton and Europa, and to study long-term phenomena such as atmospheric changes on Jupiter, Saturn and Neptune.

This important flight validation will enable radically different missions with significant onboard decision-making and novel science concept (onboard decision making and selective data return). These radical changes in mission philosophy, discarding redundant data, will enable future NASA missions to achieve significantly greater science returns with reduced resource cost.

1.1 Autonomous data processing: an introduction.

Historically, satellites and unmanned spacecraft carrying out remote sensing have made observations of selected targets and environments and have returned the complete observations for processing by researchers on the ground. To overcome the restrictions imposed on the volume of data that ASC can return and to maximize mission science return, ASC will demonstrate two autonomous data-processing technologies. The first is *autonomous change detection.* Unless change is detected from a comparison of current data with historical data (and these can be from any instrument, regardless of the wavelength range observed) there is no need for further processing of the current dataset. If change is detected, then the observation attains a high priority, as do subsequent observations to monitor change. To overcome the restrictions on data downlink (where it may not be possible to return the entire raw dataset) a much smaller processed science product can be returned: for example, if one is monitoring the open-water area on a defrosting lake, the important parameters that is needed is the position of the boundary between water and ice. This is a much smaller dataset than the whole image. In cases of even more severe downlink restrictions, only the number of pixels containing open water need be returned, allowing quantification of the rate of melting of the ice. If no change is detected, then the data is redundant and can be discarded. Only a "no change" signal is returned.

The second autonomous technology is *autonomous feature detection*, the ability to search an image for a specific pattern or object. We use the *Diamond Eye* system developed at the Jet

Propulsion Laboratory to search for specific distinct features, such as lava cones, sand dunes and impact craters. This powerful technology has widespread applications for processing remotely-sensed data on Earth and throughout the Solar System.

Both autonomous change detection and feature identification (Diamond Eye) are discussed in detail in this study.

1.2 The Autonomous Sciencecraft Constellation

The ASC experiment will fly on Techsat-21, a technology demonstration mission that is part of the larger Techsat-21 Technology Program. The Techsat-21 mission, scheduled for launch in July 2004, consists of three free-flying spacecraft (Figure 1) in a reconfigurable constellation. ASC will fly in a circular orbit, with an orbital inclination of 28.5 to 40 degrees: although not yet set, the inclination is most likely going to be 40 degrees. The approximate altitude for the constellation is 600 km, resulting in a 90-minute orbit. The principal instrument for the mission is X-band radar in each spacecraft. The radars are configurable in various modes. Most relevant to our experiment are: 1. a spotlight mode where the spacecraft all point to a specific location as they pass by; and 2. a strip map mode where the spacecraft observe a track parallel to the ground track (and which may be adjacent to each other). The radar resolution is of the order of 2m (along track and cross track)), enabling a wide range of science applications. The X-band wavelength is useful for detecting changes in small-scale surface roughness, distinguishing water from soil, and measuring high-resolution topography, thus enabling many science applications.

The Techsat-21 constellation will be demonstrating a novel radar configuration in which all three spacecraft radiate and receive simultaneously using quasi-orthogonal waveforms to enable deconstruction of the received signals into components from each of the three transmitters. While this capability will enhance our experiment by enabling acquisition of interferometric data, our experiment is designed to operate independently of the success of this instrument mode. The Techsat-21 mission is extremely downlink constrained. Two minutes of operation of the radar instruments produces approximately 33.5 GB of raw data, which would take approximately four days to downlink (even it could be processed), under most circumstances an impossible monopoly of resources. The simplest way of overcoming this bottleneck is to process the data onboard and return products rather than data. This ensures that the science content of data returned is maximized. Onboard data processing and scientific analysis means that there is no need to return the raw datasets, which can be discarded. The advantages of this process are discussed in section 2.1.

Using GPS, the constellation will have extremely accurate positioning information (required 1 cm relative and with a goal of 3 mm relative). Each of the three spacecraft in the Techsat-21 constellation has a general-purpose flight processor (an estimated 175 MIPS PowerPC with 128 MB RAM) and a payload processor (33 MHz Rad6000). The general flight processor currently has significant margin available for experimentation (only 10% of the CPU is allocated to low level basic flight software). The payload processor is expected to be in use only during and immediately after data takes. There is a slow (128Kbps) cross-link for inter-communication between spacecraft.

The basic ASC concept is shown in Figure 2. First, the spacecraft makes a science observation of a target of interest: for illustrative purposes we consider a volcanically active region, which could be on Earth, Io, or elsewhere. Onboard Science Software forms the radar image and compares it to previous images to detect whether active volcanism is taking place (new flow or deposits are observed). If an event is detected, the science module requests a new, high-resolution observation centered on the active region. The onboard planner is tasked to fulfill this request and

develops a plan to reconfigure the constellation and image the site on the next repeat orbit. The data are down-linked at the first available opportunity. The cluster management software and execution management software then ensure correct implementrvation plan.

The science experiment will demonstrate the Autonomous Sciencecraft Constellation concept grounded in a range of science experiments involving (1) change detection (relevant to scientific topics of volcanism, floods, and ice melt), all with extraterrestrial analogs; and (2) structure extraction in distributional data (e.g. volcano hypsometry). The technological improvements this mission utilizes will increase both the volume and quality of science per bit of data returned. In searching for a subset of data that has already been analyzed onboard, only relevant, useful data are returned, circumventing data transmission restrictions that prevent the downlink of full, large, raw data sets. This capability is important for two reasons. First, an expanded Solar System exploration program will place a heavy burden on the Deep Space Communications Network. It will not be possible, or even desirable, to return all data collected by a spacecraft or constellation of spacecraft. Second, missions at great distances from Earth, in hazardous environments (a Europa ocean, or the high-radiation environment of Io) will need a high degree of automation to both operate and choose which data to return.

2.0 A New Way of Doing Business: benefits of the new technologies

2.1 Increasing science return per downlinked byte.

With restrictions on the amount of data that can be downlinked, it is important to maximize the science content of each byte of data returned. For base-mission purposes, data storage and return will be pre-planned to maximize on-board storage resources. For many base mission targets it will not usually be possible to store full data sets for extended periods of time, for example, looking at seasonal changes. Instead, unit boundaries can be stored and used for the basis of comparison. The boundary files are considerably smaller than the total image, and so many such files can be stored. Base mission images (but not boundary files) can be overwritten by higher priority images. Returning the relatively small boundary files allows the full science content of the data to be extracted and returned at a greatly-reduced cost in resources. Two examples are shown below of how, through onboard processing, ASC increases science return per returned byte. In the event of severe downlink constraints, it is possible to return a single number from an analysis, such as the total new area of flow coverage, or open water, that can enable further science analysis.

Example 1 Volcanoes: Hawai'i, flow emplacement

area of interest (flow area)	2×10^5 m^2.	1.6 Mb
total image area	30×10^6 m^2.	240 Mb
size of flow boundary file		60 kb

With the emplacement of lava flows in Hawai'i, much of the science content of the data can be expressed in a file containing the location of the new flow boundaries. This information can be used as input to models to determine volumetric eruption rates and flow physical parameters. The derived boundaries can be used for comparison with existing DEMs and ground-truth data. The boundary file contains all of the information needed to do this. The file size is less than 0.1% of the

original image. Data products as a function of available downlink are shown in Table 1 in order of increasing downlink restriction. With no restrictions, product 1 can be returned, but only the higher number products can be returned in the extreme case of severely limited downlink.

Table 1. Returnable products as function of available downlink.	
1.	Raw data image of target swathe, multi satellite, single-look, complex (for ground-based interferometric processing and other analyses)
2.	Raw data image of target swathe, single satellite, single look, complex
3.	Raw data of area where change is detected, and boundary position
4.	Decorrelation map from compared images
5.	Boundary of area change (new area =dA) and flow thickness (measured or assumed)
6.	Emplaced volume (dA * thickness)
7.	Areal coverage rate (dA/dt)

Knowing the rate of areal increase, flow volume, and location of the flows is sufficient information to allow modeling of the emplacement process, aided where possible by existing DEMs. For example, knowing any two of products 5, 6 and 7 allows estimation of the third. These parameters are then used in models of eruption processes (e.g., Pinkerton and Wilson, 1994) to deduce other eruption parameters.

Example 2 Lake ice formation and breakup

area of interest (lake area)	1×10^8 m^2.	800 MB
total image area	2.4×10^8 m^2.	1.9 GB
size of flow boundary file		20 kB

To study the breakup of ice on a lake on Earth (or evaluate flooding on Europa) it is not necessary to return an entire dataset. A calculation of the change in water/ice or land water boundary, either as a pixel sum of changed area or segmented boundary file yields rates of ice formation or breakup. Again, the returned science product is a fraction of the original image data file size.

One constraint on the size of the images collected is the rate at which data can be transferred onboard from receiver to storage: transfer rates are 460 kbyte per second. With one second of operation 80 MB of data-are collected by each radar. With a resolution of about 2 m/pixel (actually a pixel coverage of 4.2 m^2), this corresponds to an areal coverage of 10 km^2, transferred from the buffer in 174 seconds. Two seconds of radar data (20 km^2, 160 MB) can be transferred in 348 seconds, and four seconds worth (40 km^2, 320 MB) can be transferred in 696 seconds, or 11.6 minutes. Combining coverage from the three satellites triples area coverage. Again, larger areas can be studied at lower resolutions.

Different process targets cover different areas. The emplacement of lava flows in Hawai'i usually covers areas of change of less than a few square kilometers. A major eruption may cover a few square kilometers, the same area as many summit calderas. Lahars cover 10's to 100's of square kilometers. Monitoring the breakup of ice on a lake depends on lake size: if the lake is prohibitively large, then data can be processed at lower resolutions. Table 2 shows typical rates of change and possible sizes of areas that may be affected by the process under scrutiny.

Table 2: Area of interest for different processes		
Process	Typical daily rate of change	Typical total area of interest
Lava flows	~0.01 to 5 km^2	10's to 100 km^2.
Lahars	10's to 100's km^2	10's to 500 km^2
Pyroclastic flows	1 to 10 km^2	500 km^2
Individual dune	< 1 km^2	10's to 1000's km^2
Windstreaks	< 1 km^2	100's to 1000 km^2
Floods: river, storm driven	1 to 100 km^2	10 to 10000 km^2
Lakes: ice formation/breakup	< 1 km^2	10-1000 km^2
Floods: dry lakes	1-50 km^2	1-50 km^2
Small impact craters	n/a	1-10 km^2
Interferometry	n/a	100-500 km^2
Volcano hypsometry	n/a	100-500 km^2 [a]

a This area is much smaller if a thin strip across the feature is selected.

2.2 Flexibility of operations

ASC demonstrates a high degree of flexibility of operations, and the ability to quickly and autonomously react to changing events as a result of on-board scientific analysis. This is a significant step beyond current spacecraft operations, where data are analysed on the ground. ASC technologies allow retargeting of resources (using the onboard planner) once trigger conditions are met (see section 4.5). ASC can react to events in real time: if a lead spacecraft in a constellation detects significant change, that information can be passed to following spacecraft which then allocate resources for more detailed (higher resolution) scrutiny of the target as spacecraft and cluster management systems allow. Such autonomous controls are a necessity in observing a dynamic process, such as rapidly changing volcanic processes on Io, dirigible operations in the atmospheres of Mars, Venus, or Titan, or control of a Europa Ocean submersible where control has to be autonomous to operate the vehicle and collect data. The description of operations in Io orbit (earlier in this report) illustrates the importance of being able to react quickly to changing observation requirements.

2.3 Impact on NASA's Future Missions: a new paradigm for Space Science

The capabilities demonstrated by ASC for autonomous command and control, resource allocation, and scientific analysis of data, represents a new way of exploring the Solar System and beyond. The science analysis techniques used by ASC, change detection and feature identification, are powerful tools that have generic applications to different datasets obtained by a variety of instruments on missions throughout the Solar System. In this section, we consider how these techniques can be used to explore other planets and moons.

NASA's roadmap for exploring the Solar System outlines future missions and required technologies to enable mission success. Onboard science data processing, as defined in this proposal, has been identified by the NASA Space Science Technology Steering Group as an enabling technology for several Exploration of the Solar System (ESS) missions including the Europa Orbiter (EO), and Pluto Express (PE) missions (see Table 3). Specifically, the feature

tracking and feature recognition technologies to be demonstrated through this proposal are considered highly enabling to these missions. The Europa Orbiter mission requires a technology demonstration to be completed by 2004. In addition, eight Sun-Earth Connection (SEC) missions and three Structure and Evolution of the Universe missions (Table 3) have identified the need for this technology.

Table 3. Planned future missions with some autonomous capability

Acronym	Mission	Time frame	Status	Theme
EO	Europa Orbiter	Near term	In strategic plan	ESS
PE	Pluto Express	Near term	In strategic plan	ESS
NO	Neptune Orbiter	Mid-term	In strategic plan	ESS
SRO	Saturn Ring Observer	Mid-term	In strategic plan	ESS
GEC	Geospace Electrodynamic Connections	Near-term	In strategic plan	SEC
IS	Interstellar Probe	Mid-term	In strategic plan	SEC
MC	Magnetospheric Constellation	Mid-term	In strategic plan	SEC
MMS	Magnetospheric Multiscale	Mid-term	In strategic plan	SEC
RAMP	Reconnection and Multiscale Probe	Mid-term	In strategic plan	SEC
RBM	Radiation Belt Mappers	Far-term	In strategic plan	SEC
PASO	Particle Acceleration Solar Orbiter	Far-term	Roadmapped only	SEC
SN	Sentinels	Far-term	Roadmapped only	SEC
ARISE	Advanced Radio Interferometry, Space-Earth	Mid-term	In strategic plan	SEU
CON-X	Constellation-X	Mid-term	In strategic plan	SEU
OWL	Orbiting Array of Wide-angle Light Collectors	Mid-term	In strategic plan	SEU

Future long-term plans include the development of a self-organizing society, a robotic colony of perhaps a hundred mini-rovers. This would have the capability to reform configurations and goals to meet changing objectives and new challenges, such as the loss of one or more components. This system would have the ability to measure the scientific worth of data, allowing low-value data to be discarded in preference to data with a higher science content.

3.0 Scientific motivation: the future exploration of the Solar System

The data analysis techniques demonstrated used to study processes on Earth can be applied to other planets and satellites in the Solar System. The applications range far beyond the processing of radar data, to other parts of the electromagnetic spectrum, searching for auroral activity on Jupiter and variability of the Io torus (ultraviolet), signs of active tectonism on Europa (visual), and volcanic thermal emission monitoring on Io (infrared). Of particular interest are Mars, Europa and Io. Missions to Europa and Mars are high-priority NASA goals: a geological mapper/volcano observer Io mission is part of NASA's roadmap for the future. Applications of the technologies demonstrated by ASC to Mars, Europa, Io, and to other missions, are discussed below.

3.1 Mars

Mars is the target of a series of missions by NASA (Mars Odyssey-2001, a Mars lander in 2003, Mars Reconnaissance Orbiter in 2005, Mars landers in 2007, Mars TelecomSat 2007/8, a competed Scout mission in 2007, a SAR-capable orbiter in 2009, and Mars Sample Return in 2011) and other organizations (European Space Agency (ESA): Mars Express; Japanese Space Agency (NSA): Nozomi, 2003). A mission with ASC capabilities will autonomously monitor ice cap change, search for windstreaks and changes in dune fields (see Figure 17), as well as search for water-related change, such as mass-wasting and debris flow processes (Malin and Edgett, 2000). Other targets of great interest would be new impact sites and areas of recent or new volcanic activity. Of particular importance is the task of landing site selection: prior testing of selection algorithms can be pre-tested on terrestrial analogs. Of particular is the gradual construction of InterMarsNet, which will yield a GPS capability. This would allow a low-cost second deployment to Mars of a variable-baseline interferometer SAR cluster.

Mars is a high priority in NASA's solar system exploration program, and orbiters or landers will be sent to Mars at every launch opportunity over the next decade. The instruments onboard these missions will be collecting more data than can be returned to Earth with the available downlink, so it is important to return only the most useful data. Onboard processing and autonomous analysis will provide the ability to determine which data should be sent to Earth.

There are many aspects of Mars that are of interest to the geological and astrobiological communities. Potential events that can be detected by an autonomous orbiter at Mars include migration of aeolian forms, ice cap expansion and retreat, freeze/thaw of martian soil, collapse of canyon or crater walls, and formation of new impact craters. Detection of these changes on a global scale without autonomous onboard analysis would be almost impossible because of the large amount of required data and limited downlink capability.

Aeolian (wind-related) features are caused by interaction of the atmosphere with the surface and provide information about the wind direction and speed at the time the features formed on Mars. For example, Viking images revealed the existence of an enormous circumpolar sand sea covering an area of ~ 7-8 X 10^5 km^2 around the north polar residual ice cap of Mars (Tsoar et al, 1979). A field of linear, transverse, and barchan dunes in the sand sea is caused by extreme temperature variations in the north polar region. During the northern hemisphere summer, these temperature variations produce strong winds that exhume materials from many sources that may include weathered lava, volcanic ash, and silicic dust. Although Breed et al. (1979) suggested that aeolian activity on Mars may have taken place early in its history, dune fields on Mars are likely archives of both ancient and recent/current wind regimes and may be markers of past environmental changes (Baker et al., 2001). Changes in aeolian features on Mars can provide clues to how active those features are today, and a method for automatic detection of those changes is the most efficient way to study the potential for changes in aeolian features on Mars.

Other processes can also provide information about the current geologic state of Mars. For example, the expansion and shrinking of the polar caps provide data on the transfer of carbon dioxide into the atmosphere. Monitoring the polar caps by returning images to Earth requires downlink of more data, whereas onboard analysis of acquired images could return outlines of ice cap extent or other less memory-intensive data. Other processes that could be monitored autonomously from martian orbit include modification of canyon or crater walls and formation of new impact craters. Also, seasonal changes at high latitudes are caused by freezing and thawing of the surface and have been observed in *Mars Global Surveyor* images. Those changes can be monitored more efficiently by an autonomous system that only returns information about the changes. Yet another

example is the dark slope streaks that have been witnessed to come into existence within a Martian year (Figure 3) [Edgett et. al., 2000]. One explanation for the origin of the features is dust avalanching, while other possibilities for some of the features include spring discharge. ASC-driven technology could be utilized to better address the origins of such enigmatic features of potential tremendous implications. The technology and science to be demonstrated by the *ASC* are required for cultivating the most information from future Mars missions.

3.2 Europa

With a radius of 1569 km, Europa (see Figure 4) is only slightly smaller than Earth's Moon and is the smallest of the four large Galilean satellites of Jupiter. The surface of Europa is covered entirely in ice and is bright with dark lineations and areas of dark, mottled terrain. The brighter regions are criss-crossed by many fractures, ridges, and other lineaments, some of which contain darker material from the subsurface. The mottled terrain is composed of chaotic areas of disrupted, iceberg-like features and darker ice that may contain a higher concentration of salts. The layer of ice/liquid on Europa is at least 100 km thick, and orbital flexing of the satellite may provide enough heat to keep part of that layer in a liquid or 'slushy' state. Intermediate and high-resolution images acquired by the *Galileo* spacecraft revealed geologically young features that suggest the presence of a subsurface layer of water or slush (Pappalardo *et al.*, 1999). The potential for a liquid water layer beneath the surface of Europa has important implications for the possibility of past or present life on Europa and for further understanding the past and present geologic state of Europa. To expand the study of that satellite, the *Europa Orbiter* mission has been proposed to use several instruments to map areas of thin ice and to learn more about the processes that formed the surface features. One instrument is a low frequency radar system that would be used to determine ice thickness. Areas of sufficiently thin ice would be considered for a future lander that would drill or melt its way through the ice to study the subsurface ocean.

Because of the high level of radiation at the distance of Europa from Jupiter, the *Europa Orbiter* spacecraft is expected to be operational for only a month after achieving orbit around Europa. The very limited time during which data will be collected makes it necessary that only the most important data be returned. Therefore, the use of onboard processing, analysis, and change detection to be demonstrated by the *ASC* mission would be very relevant to the *Europa Orbiter* mission. The ability to process data onboard the spacecraft to determine which data should be returned to Earth will enable the *Europa Orbiter* mission to maximize efficiency in its study of the distribution of thin ice on Europa.

Specifically, the direct sciencecraft onboard science processing described in this report has numerous applications to Space Science Missions. For example, in the Europa Orbiter and lander missions, onboard science processing could be used to *autonomously* monitor for (a) surface change as function of changing tidal stress field; (b) monitoring areas of greatest tidal stresses; (c) search for surface change, evidence of recent activity; and (d) search for landing sites which have a high probability of lander survivability and where the crust is thin for deployment of a sub-crust submarine explorer.

3.3 Io

A dedicated mission to study Io (the Io Volcano Observer) is part of NASA's roadmap for exploring the Solar System. Io is the innermost of the four Galilean satellites orbiting Jupiter, and is

most volcanic body in the Solar System. It is the only extraterrestrial body in the Solar System where high-temperature (> 1000K) volcanism is being observed. Io's surface is covered in lava flows and other volcanic deposits, and pockmarked with deep volcanic calderas. Deposits from large volcanic plumes, rich in sulfur and sulfur dioxide, and which can extend hundreds of kilometers above the surface, lay down deposits over a thousand kilometers across. Orbiting deep within Jupiter's magnetosphere, Io is an intensely hostile environment for a spacecraft, receiving a radiation dose of 4Mrad per day. As a result, an orbital mission to Io would be brief. Even a spacecraft in Jupiter orbit would rapidly build up a large radiation dose through repeated Io encounters. Under such operational constraints it is therefore vital to identify and collect the most valuable data from short-lived but important volcanic episodes such as fire-fountain events. Autonomous operation is necessary to maximize the opportunities that are unlikely to be observed again due to their rarity or the short duration of the mission.

Io was imaged by the Voyager spacecraft in 1979, and since 1996 has been regularly observed by instruments on the Galileo spacecraft. Many changes on the surface have been identified on time scales from decades (Voyager to Galileo, Figure 5a,b) to a few weeks (Figure 5c,d) and on spatial scales ranging from a few tens of meters to over 1000 km (Figure 5e,f). Recent analyses have allowed rates of areal increase of lava flows to be determined (Davies et al., 2000; McEwen et al., 2000; Keszthelyi et al., 2001) and estimates of volumetric eruption rate to be made (Davies et al., 2001; Davies, 2001). Some of the lavas on Io are at extremely high temperatures (>1800 K, McEwen et al., 1998; Davies et al., 2001), indicative of ultramafic volcanism. Io is therefore an analog for the early Earth, where widespread ultramafic volcanism has not occurred for aeons. The change detection techniques employed by ASC for observing volcanism on Earth can easily be applied to Io. Autonomous detection of active volcanism is a significant advance beyond current Galileo operations, where at high spatial resolutions, targets of interest are selected well before the encounter in the hope that something interesting will occur at time of observation. An autonomous change detection algorithm can be used to search for specific thermal or visual-wavelength targets.

An Io-dedicated mission (such as the proposed Discovery-class *Volcan* mission) would investigate volcanic phenomena which have a direct bearing on understanding the evolution of the Earth. Building on what has been learned from studying terrestrial volcanoes, and past missions to Io, *Volcan* would map the changing shape of Io's volcanism, measure tectonic stresses at global, regional, and local levels; and detect and quantify surface feature planform and topographic change. Additionally, a high degree of autonomous operation is necessary with an Io observer to allow real-time target switching, if a high-priority, transient phenomenon occurs (for example, an explosive fire-fountain event, with a lifetime of order minutes to hours).

Another important experiment enabled by the technology on ASC is autonomous impact crater detection. Io is unique in that no impact crater has been identified on the surface, a testament to the extremely high rate at which the satellite is being resurfaced. With Io, and every other solid body, constant monitoring of the surface and comparison with the way the surface looked during the last observation will allow fast identification of new craters, land slides, lava or pyroclastic flow emplacement: in fact, any kind of planform change will be detected.

3.4 Other missions: Venus, Titan, and beyond.

3.4.1 Venus.

Venus is covered in a thick, opaque atmosphere, which is best penetrated using radar. The Magellan mission to Venus was one of NASA's greatest triumphs. The Magellan radar unveiled Venus to show a young volcanic landscape (Figures 6). Radar was the only way to globally map the surface in such detail (Figure 7). A subsequent mission satellite cluster (similar to ASC) would initially search for evidence of change through comparison with Magellan data, with the option to reconfigure for high-resolution observation of areas where change has occurred. This type of change-monitoring mission would be beneficial to a proposed NASA Venus Surface Sample Return mission.

3.4.2 Titan

The autonomous technologies described in this report can also be applied to Titan, the largest satellite of Saturn. Like Venus, Titan is covered by a thick, visually-opaque atmosphere. The Cassini-Huygens mission may reveal whether or not Titan has oceans. A radar-mapping mission (as part of Titan Organic Explorer) can penetrate the cloud cover (as with Venus) and map the surface. After target selection, high-resolution interferometry can be used to monitor coastline/boundary changes. Studies are in progress to develop airborne rovers that will explore Titan (Figure 8).

3.4.3 The Gas Giants and their satellites

The atmospheres of Jupiter, Saturn, Uranus, and Neptune can be constantly monitored for evidence of change (Figure 9), allowing identification and tracking of weather systems. By comparing images and temperature maps, the evolution and behavior of individual systems can be followed, and an analysis of the data, such as analyses of wind velocities and temperature variations, will be returned. New features, such as the enigmatic "brown barges" and white spots on Jupiter, can be identified for closer study. As part of the Neptune Orbiter mission, cryogenic volcanism could be studied on Triton (Figure 10) using change detection and pattern recognition technology. This would enable tracking of active nitrogen plumes, resurfacing by flows, changes in seasonal ice caps, and windstreaked deposits indicative of widespread volcanism, on Triton.

3.4.4 Other missions

The establishment of robotic colonies on Mars has already been discussed. Such an undertaking, with a wide range of rovers both on and above the surface of Mars, will by its nature need to operate autonomously. The massive amount of data generated will need autonomous processing to extract science content, which will in part be used to determine subsequent colony operations. ASC is a step on the road to achieving this level of autonomy. The ASC mission (and therefore the thrust of this report) is primarily interested in planetary science, searching for geomorphologic or environmental change on the surface or in the atmospheres of planets. However, the techniques of autonomous data analysis can be just as easily applied to other missions exploring the solar and interplanetary environment. The benefits of such an autonomous capability are discussed in the next section of the report.

4.0 Earth science with ASC

4.1 Observing Earth with Synthetic Aperture Radar

Techsat-21 provides an excellent mission on which to demonstrate the utility of our change detection and feature identification technology. Synthetic Aperture Radar (SAR) has become a powerful tool to observe Earth, with a number of highly successful missions flown in the last 10 years. Table 4 shows some details of previous orbital and airborne missions that have observed the Earth with SAR. The SIR-C/X-SAR missions were highly successful, observing many targets and a wide range of physical processes. For example, the first SIR-C/X-SAR mission, in April 1994, collected a total of 65 hours of data during a10 day period, roughly corresponding to 66 million square kilometers. All data were stored onboard the shuttle using a new generation of high-density, digital, rotary-head tape recorders. The volumes of data were so large that transmission to Earth was impossible, and so the data were stored onboard the shuttle. The April 1994 mission data filled 166 digital tape cartridges (similar to VCR tape cassettes). Twenty-five of those tapes were filled with X-SAR data, a total of 47 terabits of data or the equivalent of 20,000 encyclopedia volumes. With a mission observing the surface of Earth, or any planet or satellite for an extended period of time, the amount of data generated is simply gigantic: this more than anything demonstrates the need to reduce data prior to transmission. The second shuttle SIR-C/X-SAR mission flew in September and October 1994, and duplicated selected mission 1 orbits to within 10 m, allowing repeat-pass targeted interferometry, a mission main goal. The second mission returned 60 terabits of data, equivalent to 25,000 encyclopedia volumes.

The Shuttle Radar Topography Mission (SRTM), a mission that used C-band and X-band inteferometric synthetic aperture radar to acquire topographic data of 80% of Earth's landmass, flew in February 2000. In 11 days over 12.3 terabits were collected, equal to the contents of the Library of Congress. Because of the large amount of data, it was necessary to return the data to Earth on data tapes for post-mission processing.

Although ASC will only be able to return a fraction of the data volume collected by SIR-C/X-SAR and SRTM, the data that are returned will have been processed onboard to extract the most scientifically useful data. With three months of operations dedicated to science in the first year of the mission and six months in the second year, the theoretical maximum data return, at 10 GB/week/satellite is approximately 1 terabyte, equivalent to raw data coverage of 125,000 km^2. Through use of autonomous onboard processing, we ensure that the most valuable data, those data with the highest science content, are preferentially returned, to maximize the total science return of the mission.

Table 4.
Orbital Characteristics of Earth-Orbiting Radar Missions

Mission	Launch/dates	Mean altitude, km	Inclination, degrees	Period, mins	Repeat coverage, days	wavelength and polarization
ERS-1	JUL 17 1991	782	98.5	100	35	5.66, VV
ERS-2	APR 21 1995	780			3	5.66, VV
JERS-1	FEB 11 1992	568	97.7	96	44	24, HH
RADARSAT	NOV 4 1995	798	98.6	100.7	24	5.6, HH
SIR-C/X-SAR SRL1	APR 9-20 1994	225	57		Various	3.1-23.5 HH,HV,VH,VV
SIR-C/X-SAR SLR2	SEP 30 – OCT 11·1994	225	57		Various	3.1-23.5 HH,HV,VH,VV
SRTM	FEB 11-22 2000	225	57			

ASC	JUL 2004-2005	600	28.5-40	90	1-3	3.5 cm
Airborne radar missions						
AIRSAR/ TOPSAR	Deployments yearly since 1990	2-8				5.7,25,68 HH,HV,VH,VV
Orbital and Mission Characteristics of Venus-Orbiting Radar missions						
Magellan	SEP 1990-OCT 1994	periapsis 294	86	3.25 hrs	243	12.6

4.2 ASC experiment types

ASC will carry out several of types of experiment: three examples are outlined below, describing change identification, feature identification and a static observation (hypsometry).

Experiment Class 1: Identifying Agents of Change.

In this experiment, onboard science processing is utilized to isolate areas of change in order to downlink only the regions of change or data quantifying the amount of change. Change in radar reflectivity will be used to identify areas of changing features. The general approach consists of several steps:

(1) consultation of target list and selection of target
(2) acquisition of radar data of target
(3) formation of radar image
(4) comparison of returned data with previously obtained data
(5) determination of presence or absence of change
(6) downlink of changed data subset (only downlink region of change)
(7) re-prioritize observation for high-resolution repeat imaging

Lossless compression will further reduce downlinked data volume. The degree of compression is likely to be high once the pattern recognition techniques are used to define areas of change. Specific experiments targeting processes of interest are described in detail in section 4.6.

Experiment Class 2: Identification of specific features.

Here, onboard scientific processing is used to identify specific objects in the datasets. These targets include impact and volcanic craters, volcanic cones and sand dunes. The feature identification algorithms are described in section 4.7 and some example targets listed in Appendix 2.

The general approach consists of:

(1) Consult target list and image target
(2) Acquisition of target data
(3) Registration of radar data
(4) Search target for specific targets using scalable target templates
(5) Determine number, scale and position of identified targets.
(6) Compare with previous data for new features (change detection)

(7) Compare with previous data for feature movement

Product 1 to be returned: Number and type of targets, feature size.
Product 2 to be returned: New features, any movement of features.

Experiment Class 3: Extraction of structure in landform data.

In this experiment type, the target is of geological significance, and static. The intent is not to capture a dynamic event, although if landform change takes place (a volcano blows off its peak, or a major landslide occurs) this product will identify it if previous analyses are available for comparison. In an example case we can calculate the hypsometry of a target, such as a volcano, yielding structural/tectonic information (see Finn et al. 1995) as a product much smaller than the full, raw dataset. This experiment would proceed as follows:

(1) consult target list and image target
(2) acquisition of radar data
(3) registration of radar data
(4) generation of elevation data from radar data
(5) calculate intersection of horizontal planes at different elevations at 1 m intervals
(6) create histogram of number of pixels and elevation
(7) determine local peaks in histogram

Product 1 to be returned: histogram data, and identification of local peaks in the distribution.
Product 2 to be returned: spatial distribution at local peaks.

This experiment could involve later comparisons against existing radar data for targets of interest such as the Mauna Loa and Kilauea volcanoes in Hawaii to look for areas of deformation. Other resources can also be utilized, such as high-resolution (~20 cm vertical resolution) digital elevation models (DEMs) of selected volcanoes [Gwinner et al., 2000].

4.4 Target-data prioritization and probability of process occurrence.

How are targets selected for observation? Firstly, processes are chosen that have observed or likely extraterrestrial analogues. Terrestrial sites where these processes occur are compiled into target lists (see Appendices 1 and 2). Figure 11 shows the targets listed in Appendix 1, which is by no means an exhaustive list of targets. Whether or not a process is actually observed during the duration of the mission depends upon the rarity of the process.

To ensure a guaranteed minimum science return from the Earth-oriented mission, a prioritized target list is compiled of observations of features, some static, and therefore guaranteed to be observed, and phenomenological, each with a different likelihood of being observed. All of these targets fall into three categories, most of which have analogs elsewhere in the Solar System. The first target category consists of *"Guaranteed Occurring Phenomena"*. The list of targets includes the Decade volcanoes (see Web links) and permanently active volcanoes (see Simkin and Siebert, 1999) that lie within the latitude limits defined by the Techsat-21 orbital geometry, as well as dune fields and lakes which freeze and unfreeze seasonally.

The second category is "*High Likelihood of Observation*". Examples include snow-cap and lake/sea ice formation and retreat (N. India, Nepal) and the relationship with flooding; seasonal flooding of low-lying areas (Bangladesh, N. India, E. China), the encroachment of desert (Egypt, Libya); and other volcanic eruptions (compared to those classified as *Guaranteed Occurring Phenomena* of higher probability) leading to the emplacement of lava flow fields (Etna, Italy)) and other volcanic products (e.g., lahars, Pinatubo).

The third category is "*Lower Possibility Observations*". Examples include major, catastrophic volcanic eruptions (Mt. St. Helens, Pinatubo: VEI (Volcano Explosivity Index) >3), 50-100-year flooding events, and major earthquakes (> 6.0 on the Richter scale).

Table 5 shows the processes ASC will observe for each of the experiments outlined above, and classified by their likelihood of occurrence. Each process is assigned an initial priority. A low-priority observation would typically be superceded by a higher-priority observation. However, once a process is observed, it is re-prioritized with a higher priority so that the evolution of the process can be observed. Seasonal-dependant processes have variable priorities as a function of time of year. For low-priority observations, priority will increase the longer the mission progresses without these observations being made. Specific targets for each process are listed in Appendices 1 and 2. The individual processes are described in sections 4.5, 4.6 and 4.7. In all cases, observation prioritization can be overridden by command from the ground should a rare event of high scientific value occur.

Table 5. Change, Feature Detection and Static Process Observation Prioritization				
Experiment 1: Change detection				
Possibility of observation	Process	Process class	Time-of-year sensitive?	Initial Observation Priority
Guaranteed	Lake freeze-thaw	ICE	Yes	Low
	Permanently active volcanoes	VOLCANO	No	Low
	Dune observation	AEOLIAN	No	Low
	Flooding (annual inundation)	FLOOD	Yes	Low
	Annual snow cap melt	ICE	Yes	Low
High	Wind streaks	AEOLIAN	No	Medium
	Dune movement, shape change	AEOLIAN	No	Medium
	Dry lake flooding	FLOOD	Yes	Medium
	Large eruption	VOLCANO	No	Medium
	Lahar emplacement	VOLCANO	Maybe	Medium
	Periglacial (permafrost) change	ICE	Yes	Medium
Low	Ice sheet breakup	ICE	Yes	High
	Decade volcano eruption	VOLCANO	No	High
	Other large eruption	VOLCANO	No	High
	Streaks: backscatter change	AEOLIAN	No	High
	Large dust storm	AEOLIAN	Maybe	High
	Major (100 yr) flood	FLOOD	Yes	High
	Lahars	VOLCANO	Often	High
Experiment 2: Feature Identification				
Guaranteed	Cones, craters	VOLCANO	No	Low
Guaranteed	Impact craters	IMPACT	No	Low
Guaranteed	Sand dunes	AEOLIAN	No	Low
Low	New eruptions	VOLCANO	No	High
Experiment 3: Static Observations (examples)				
Guaranteed	Interferometry data	VOLCANO	No	Low
Guaranteed	Hypsometry	VOLCANO	No	Low

Aeolian process targets are listed in Appendix 1 in order of decreasing priority. The highest priority for aeolian features is detecting migration of individual dunes. This information is important for understanding the speed at which dunes migrate and is best acquired autonomously without many hours of analysis on the ground. The second priority for sand dunes is detecting change in the planform shape of the dunes. These changes could be caused by physical obstructions and provide information about how dunes evolve.

The first priority for wind streaks is detecting changes in the planform shape of the streaks. These changes could signify an increase or decrease in size of the streak and could be due to changes in sediment supply or wind pattern. Change in orientation of the streak is also important and would be caused by a change in the wind direction. The second priority for wind streaks would be

detection of a change in the backscatter of the streak caused by changes in the thickness and distribution of the sediment.

It is likely that the high resolution of the *ASC* radar will be able to detect small changes in the locations of at least some of the barchan dunes targeted in this study. Although it is less likely that change will be detected in the wind streak orientations, changes in their backscatter could occur within the length of this mission.

Certain areas of the world are prone to flooding, on predictable cycles. Possible targets include the Manaus region of Amazonia in Brazil, and areas of Bangladesh and southeastern China. Rare events, such as 100 year floods, are designated a high-priority processes in order to determine the evolution of the event. Additionally, ASC can monitor smaller dry lakes that seasonally flood. Flood prediction models, based on past occurrence and meteorological forecasts can be used to determine areas likely to be affected by flood events: this will enable pre-flood observations to be made for later comparison.

The highest priority for the study of ice is detection of ice deformation when little open water exists. Such deformation would occur when currents within large lakes (or the ocean) cause movement of the ice or when continued ice growth results in compression of the ice. Deformation within the ice is the priority because it is important to understand such deformation so that areas of weakness can be exploited for shipping lanes in high latitude regions. Autonomous detection of ice deformation also has important implications for the future *Europa Orbiter* mission. The second priority in ice formation and retreat is distinguishing between the areas of ice and water. There is the highest probability that ice will form and thaw in the target areas during the yearlong mission. However, it is difficult to predict the degree of deformation that will take place in these moderate-size lakes.

4.5 Generation of onboard products: triggers and reactions

A series of actions are triggered by the onboard data processing software. The triggers and reactions are shown in Figure 12. On the left are shown the trigger events driving acquisition and processing of data, and on the right are shown the reactions. In cases where it is not possible to store large image datasets of a large lake, a product such as a segmented boundary containing the locations the water/ice boundary.

4.6 ASC change detection science experiments

This section describes in more detail the different terrestrial target types (see section 4.4) representing environmental and geological processes that can be detected and monitored by ASC. How each process will be observed by ASC is described, as is the significance of the science product that will be returned, and the anticipated results. Each process has observed or high-probability extraterrestrial analogs.

4.6.1 Ice formation and retreat

Radar is a unique tool for studying the development and retreat of lake ice and sea ice. Radar data provide information about the thickness and extent of ice cover, which is important in understanding the effect of ice cover on the global climate. Understanding when lake ice begins to break up can help determine when water navigation can begin and when spring runoff will replenish water reservoirs (Williams, 1965; 1970). Information on ice thickness and locations of open water is also important for determining shipping lanes through polar regions and ice-packed lakes and rivers.

In large lakes and in oceans, currents cause deformation of the ice and translation of ice blocks that occurs over a period of hours.

Previous radar sensors (*e.g. RADARSAT* and *SIR-C/X-SAR*) have returned images showing the formation of ice, its modification, and its eventual retreat. The April and October 1994 *SIR-C/X-SAR* missions imaged several locations of sea ice, lake ice and frozen rivers with multi-frequency radar showing daily changes in the arrangement of ice blocks and in the amount of open water. *RADARSAT* has been especially successful in returning images of sea ice in the polar regions because of its polar orbit and frequent repeat-pass times. ASC will expand the successes of these previous radar missions by targeting ice formation and retreat at a resolution of ~2-meter and a repeat pass of 3 days. In addition to helping understand ice processes on Earth by targeting high-elevation lakes, the ASC mission will be a precursor to the *Europa Orbiter* mission that will use a radar sounder to identify areas of thin ice on Europa. For that mission, onboard processing and analysis will be crucial for returning the most useful data.

ASC Ice Formation Experiment Examples

The seasonal cycle of ice formation and retreat will be studied with the ASC in order to demonstrate the usefulness of automatic detection of changes in ice coverage and arrangement of ice. On Earth, most ice occurs in the ocean and in lakes at high latitudes, but because the ASC will probably not be in a high-inclination orbit, radar images of formation and break-up of sea ice will not be acquired. Therefore, high elevation lakes will be targeted to study ice formation and retreat on a smaller scale to demonstrate how autonomous processing can be very useful for detecting and tracking changes in ice cover.

Examples of high elevation lakes in India that will be targeted during the ASC mission are shown in Figure 13. Both lakes show ice cover (higher backscatter likely due to rough ice or air bubbles (Swift *et al.*, 1980; Leconte and Klassen, 1991)) in the April images but open water in the October images. The April images show the winter ice still present on the lake, and the ice might be in the process of thawing because some open water is visible in both images. The October images show the lakes before they have begun to freeze for the winter. During the ASC mission, the targets for ice will be monitored frequently so that initial ice formation can be detected and tracked. Once change is detected, ice growth will be tracked often, and outlines of the water/ice boundary will be generated onboard and returned to Earth. Once a lake is covered entirely by ice, outlines will only be generated if change is detected. For each outline returned, the option will exist to return the image of the change before it is deleted from the onboard memory.

As the mission progresses, the ice will begin to thaw and break up. These changes will again be monitored closely to understand how thaw and break up of ice compares to ice formation. The results from ASC will be used to further understand the frequent changes during ice formation and retreat without the need to process many radar images on the ground. These results can be tied to models of ice growth and can be related to larger areas of ice such as sea ice.

4.6.2 Volcanoes

Volcanoes continue to shape the surface of Earth and other bodies in the Solar System. Understanding volcanoes and environmental interactions is important for a number of reasons: volcanoes are surface expressions of internal processes, and local and global climate can be affected by volcanic eruptions, or even a single eruption if large enough. Most importantly, volcanic activity may be hazardous to those in the vicinity of the volcano: both on the ground and in the air: it has

been estimated that in the last two decades $250 million of damage has been caused to aircraft by volcanic ash and pyroclastics (Simkin and Siebert, 1999). Due to remoteness, difficult terrain, or the inherent danger of in-situ investigation, remote-sensing is often the only way to observe and monitor a volcano.

The appearance of volcanoes in radar images is controlled primarily by two terrain characteristics: topography and surface roughness. Steep volcanic slopes can strongly reflect radar waves if the incident wave hits the slope at a near perpendicular angle. The slopes of volcanoes, and volcanic cones, domes, craters and flows are a function of composition and eruption style, and strongly reflect radar waves. Variations in surface roughness of volcanic flows and deposits are also discernable: a surface will appear bright if it is rough on a scale comparable to the radar wavelength. In the case of ASC, the X-band radar wavelength is of the order of 3 cm. Basalt lava flows, the most common on Earth, occur in two roughness textures: a'a, which has an extremely rough, blocky texture, and pahoehoe, which has a smoother, more rounded texture. Ash deposits and lahars also have different textures. Smooth, fine-grained ash deposits appear dark to the radar while deposits with larger fragments may appear "rough", and therefore brighter at some wavelengths. The emplacement of new material leads to decorrelation of data in these areas when before- and after-observations are compared. In the case where lava flows cover areas with a very different radar reflectance, pattern recognition algorithms can determine the new area covered.

ASC Volcano Experiment Examples

During the ASC mission we will monitor selected volcanoes for signs of change, primarily the emplacement of new lava flows, lahars and pyroclastic flows. If change is detected ASC will autonomously determine areal coverage rates and, in the case of lava flows, volumetric eruption rates, the most important eruption parameter. These data can then be used in mathematical models of volcanic processes, where possible, in conjunction with digital elevation models (DEMs), to derive other eruption characteristics. Additionally, an experiment determining volcano hypsometry can be performed, returning a science analysis of the data without the need to return the entire dataset itself. Two targets of interest and specific experiments are described below.

1. Lava flow emplacement at Kilauea, Hawai'i.

Kilauea is the youngest volcano on the island of Hawai'i and is, with Mauna Loa, a high-priority target. To a volcanologist, Kilauea has two great advantages over many of its peers: it is easily accessible, and has been almost continuously active since 1983. Previous radar missions have also targeted Kilauea and the Hawaiian Islands. In particular, the Shuttle Imaging Radar-C/X-band Synthetic Aperture Radar (SIR-C/X-SAR) missions in 1994 returned a wealth of data of many volcanoes, including Kilauea (Figure 14). More recently, AIRSAR collected data of Kilauea and other volcanoes and islands during the PACRIM-2000 deployment. High-resolution DEMs also are being produced from the data collected during the Shuttle Radar Topography Mission (SRTM) in 2000, which should be available by Techsat-21 launch. Other high-resolution DEMs are in production from aircraft data (Gwinner et al., 2000). De-correlation of SIR-C data of Kilauea has been used to determine the rate at which lava flows are emplaced, on a day-to-day basis, as demonstrated by Zebker et al. (1996), and shown in Figure 15. The emplacement of new lava results in a change in local topography, and therefore a change in phase in exact-repeat track observations, if the depth of the new lava is greater than the wavelength of the observing radar. Decorrelation of the images reveals the newly emplaced areas. In the case where downlink

resources are at a minimum, only the area of the new flows, and an averaged rate of emplacement, need be returned to enable further scientific analysis. Kilauea has the advantage of easy access: we will locate field teams specifically for the purpose of supporting these radar observations. The comparison between ASC-derived analyses and ground-truth will aid interpretation of data from locations where such ground-truth is unavailable.

2. Pyroclastic deposits and lahar emplacement, Mt. Pinatubo, Philippines.

The same techniques used to determine lava flow emplacement parameters can be applied to other considerably more dangerous volcanic processes, such as lahars (mud flows of melted ice and volcanic debris or remobilized ash deposits) and pyroclastic flows that show up readily in radar images (see Figure 16). Few eruption products are as deadly, and although they are rare events many volcanoes have the potential to produce lahars. The worst-case scenario of a major eruption in proximity to a population center occurred at Mt Pinatubo in the Philippines in June 1991. The eruption produced about 5.5 cubic kilometers of pyroclastic-flow deposits, an order of magnitude greater than the volume of magma erupted in 1980 from Mount St. Helens. Pyroclastic flows traveled as much as 12 to 16 kilometers from the vent, impacted directly an area of almost 400 square kilometers, and profoundly altered the landscape. In proximal areas, flows were highly erosive and left little deposit, but, in medial and distal areas, they created broad, thick valley fills and fans of ponded pyroclastic-flow deposits as well as veneers on ridges and uplands. Even after the eruption had ended, the large, unstable ash deposits, easily mobilized by monsoon rains, have every year posed a significant threat. AIRSAR observed the emplacement of new lahars emplaced during the 2000 monsoons (images are available through the JPL AIRSAR website). ASC will monitor existing high-risk areas and other eruptions to monitor both pyroclastic flow deposits and lahars.

4.6.3 Aeolian forms.

Global wind regimes are related to the pressure differentials associated with planet-wide circulation patterns. In contrast, physical characteristics within a specific area or region generate local wind anomalies. Local wind anomalies are often observed in those environments where large temperature variations exist in the air layer immediately above the ground, and such conditions are common in deserts, along seacoasts, or in areas with pronounced diversity in elevation. Wind-scoured landscapes and wind-deposited landforms are often the result of the direction, velocity, and degree of turbulence of wind. Thus, wind-related features (*e.g.*, sand seas, dunes, and streaks) are not only markers of present-day circulation patterns and local conditions but may also archive past conditions. Therefore, remote observations of wind-related phenomena coupled with ground truth are necessary to improve our understanding of wind-related processes and to help unravel past climatological conditions on Earth and other planetary bodies.

Imaging radar is useful for studying aeolian forms such as sand dunes and wind streaks that provide information about the regional and local wind regimes. Low-frequency radar has the ability to penetrate several meters of dry sand (*e.g.*, McCauley *et al.*, 1982), but higher frequency radar cannot penetrate as deeply and is absorbed by thick sand deposits. This makes X-band radar appropriate for investigating the migration of sand dunes and changes in wind streaks. Dune migration typically occurs over the time scale of years, but monthly (and seasonal) changes may be detected using high-resolution images. The *SIR-C/X-SAR* mission provided images of migrating barchan dunes in desert areas with active aeolian processes, but no change could be detected between the April and October missions because such changes were not resolvable at the resolution

of *SIR-C/X-SAR*. The high resolution of the ASC radar system will enable detection of changes in aeolian features on Earth over the period of a year. Autonomous detection of changes in aeolian forms on Earth will provide necessary experience for future missions to Mars that would have the potential for automatic detection of active processes.

ASC Aeolian Experiment Examples

Aeolian features such as dunes and wind streaks can exhibit small changes over the period of a year. These changes can be the migration of a dune, seasonal changes in the slip face of a dune, or changes in sediment thickness in a wind streak. Changes in the location or form of an aeolian feature provide information about the local wind patterns and can be used to understand how quickly (or slowly) a dune is moving toward features such as houses, highways, or railroad lines. The high-resolution of the ACS images will allow change detection of sand dunes and wind streaks within the latitude range covered by the spacecraft.

Examples of sand dunes chosen as targets are barchan dunes (crescent shaped) in Chad and Egypt (Figure 17) that occur in areas of strong winds, making these dunes good candidates for displaying changes over the yearlong ASC mission. The barchan dunes should keep their general shape during the mission, but small changes in their location will be detected by the ~2-meter resolution of the ASC radar system. Images of the dunes will be compared to images acquired at the start of the mission, and the onboard software will determine if change in the shape or location of the dune has occurred. If change is detected, outlines of the dune before and after the change will be returned from the spacecraft for analysis. Depending on the length of time it takes to detect the change, dunes that exhibit change will be classified as priority aeolian targets for the remainder of the mission.

Wind streaks will also be imaged to detect changes in streak appearance due to redistribution of sediment. Although good examples of streaks in Bolivia and Syria (Figure 18) were imaged during the SIR-C/X-SAR missions, images were only acquired during one of the two flights so no change could be detected. It is expected however that continued wind processes would produce changes in the sediment distribution that would cause a change in the backscatter of the streak. Detecting change in wind streaks is necessary for understanding changes in the wind pattern or speed over time and for monitoring transport of material. If a change is detected during the ASC mission, portions of the wind streaks showing the change will be returned from the pre- and post-change images so that the changes in backscatter can be compared to experimental measurements to estimate the change in sediment thickness.

4.6.4 Floods

An often-catastrophic terrestrial event, flooding shaped the surface of Mars in the distant past and may be important surface process on Europa and Titan. On Earth, satellite-based flood detection provides important information for governmental agencies monitoring disasters [Rao et al., 1998] and supplies data to scientists seeking to understand the responses of surface processes to storm events at synoptic scales. Some of the most important hydrological phenomena occur in transient fashion and at arbitrary times over regions of varying scales. Major floods, such as those that have devastated parts of the world (e.g., major flooding from Hurricane Mitch resulted in tremendous loss of life, major structural damage, and notable modification of the landscape in parts of Central America), comprise phenomena that can be readily sensed from orbital radar platforms to improve the scientific understanding necessary to mitigate their disastrous consequences (Figure 19).

Channels are the primary conduits for water, sediment, and dissolved load for both Earth and Mars. On Earth, the aerial extent of these conduits varies with the seasons and with inter-annual climatic fluctuation: rivers may be nearly dry during times of drought, and then expand to inundate valleys many tens of kilometers wide during wet seasons or during flood events [*Hirschboeck, 1987*]. The largest terrestrial floods in a specific location are linked to processes occurring globally by means of large-scale connections among climate, ocean, and hydrologic dynamics [*Hirschboeck, 1991*]. On Mars, the calculated peak flow magnitudes, for example, are comparable to those of the high-discharge western boundary currents of Earth's world ocean, such as the Gulf Stream, the Kuroshio, and the Agulhas [*Baker, in press*]. Until recently, remote sensing of river floods were constrained by low spatial resolution and cloud cover, which made it impossible to obtain data during the initial stages of most large events [*Brakenridge et al., 1994*]. The cloud-penetrating C-band synthetic aperture radar (SAR) on board the *European Remote Sensing* (ERS-1) satellite (as well as ERS-2) removed both of these constraints [*Brakenridge et al., 1994*]. SAR penetrates cloud cover and affords a view of the surface even during flooding, a requirement for direct observation of flood inundation.

ASC Flood Experiment Examples

Flood-induced changes include: (1) varying depositional surfaces with contrasting radar reflectances (e.g., gravel deposits, conglomerates of meters-size boulders, gravels, and smooth slackwater deposits), resulting from several factors such as stream velocity, peak depth, channel geometries, tributary densities, etc., and (2) erosional scars, including anastomosing channel patterns, streamlined islands, longitudinal grooves, and inner channels. Large storm systems during the ASC mission are possible precursors of floods: forecasts may be used to update ASC target lists to obtain pre-flood target observations. ASC products will mostly consist of areas of change and rates of areal change, as well as pre- and post- topography to determine erosion rates. The results of scientific analysis of the floods, using computer models of flow and flood processes in conjunction with existing DEMs will enable detailed post-mission reconstruction of the event and may lead to a better understanding necessary to mitigate the consequences of floods.

Analysis of 3 day repeat track ERS-1 SAR images allowed a flood evolution cartography with sufficient accuracy for a field process analysis and enabled an accurate description of flood dynamics of the 1993 and 1994 floods in the Camargue region, France (e.g., Figure 20) [Laugier et al., 1998]. Although outside of the ASC latitude range, this is a fine example of a technique that can be used elsewhere. The comparison between this method and conventional mapping techniques indicated usefulness of SAR data in producing a quick and effective cartography of flood evolution. Since the ERS-1 three-day repeat track operational mode was only temporary, all these results show great potential of high temporal resolution SAR data acquisitions by ASC. After data have been returned to the ground, the coupling of the SAR data with digital terrain models is a useful approach in the determination of the current and future extent (through modeling) of flooded areas. Flood targets are shown in Appendix A1, and include areas of S.E. Asia and South America. Other flood detection targets are dry-lake beds, mostly in Southern California that occasionally flood in winter. These lakes are generally of the order of a few to 10's of km^2 in area, well within the processing capabilities of ASC, and providing excellent targets for change detection and process monitoring.

4.7 The ASC feature detection experiment: Diamond Eye.

4.7.1 Overview.

Other than change detection, the other major technology demonstration is that of feature identification, the ability to use an autonomous data processing system to search for and find specified targets. The Diamond Eye system (Burl et al., 1999) came about as result of the recognition that while the amount of data being returned from planetary missions was increasing, the ability of humans to manually process it was not, and that placing intelligent algorithms onboard a spacecraft would enable new science opportunities that could not be realized with existing technology.

The Diamond Eye Project targets development of a suite of algorithms that will enable both scientists and remote systems to find, analyze, and catalog spatial objects and dynamic events in large scientific datasets and real-time image streams. The algorithms are integrated into an innovative image data mining architecture. Algorithm types are as follows:

(1) Adaptive recognition. These are recognition algorithms that can be easily trained to new domains without reprogramming. Typically, these algorithms rely on machine learning techniques to automatically abstract a model from user-defined training examples.
(2) Ad Hoc Queries. Although the use of learning techniques usually depends on an abundance of training examples, it is often desirable to search for objects based on a single example, or even a notional concept of what the object might look like.
(3) Discovery. As spacecraft venture to new environments where we cannot know what to expect in advance (Pluto, Europan sub-surface, Titan, microscopic views of Mars) generic discovery algorithms that can autonomously identify "interesting" objects with no prior model will be invaluable for improving scientific return.
(4) Dynamic events. Algorithms for detecting and tracking dynamic events in image sequences can exploit both spatial and temporal behavior. For applications with significant spatial structure the adaptive recognition techniques can be modified to incorporate temporal aspects.

4.7.2 Applications.

Diamond Eye will be used to autonomously search data for specific geomorphological features and then return the locations of the targets. Applications include automated impact crater and volcano detection.

Diamond Eye has been trained to recognize the circular patterns of impact craters (Burl, 1999) a nearly ubiquitous landform on the terrestrial planets and most moons in the solar system. The exception is Io because of its volcanically active surface (see Section 3.3). Impact craters form through well-understood hyper-velocity impacts, producing process-unique morphologies. Figure 21 shows the results of running Diamond Eye on a Mars image, identifying impact craters (green boxes). During the ASC mission, impact craters (such as Wolf Creek crater, Western Australia, and Meteor Crater, Arizona) and similar targets, such as cinder cones and barchan sand dunes, will be searched for on Earth (Figure 15) using Diamond Eye.

Diamond Eye has been used also with great success to identify dome volcanoes in Magellan radar data of Venus (Burl et al., 1998), wind streaks on Mars, and dune features on Earth. As Diamond Eye relies on specific orientation of target templates, and also scalable templates, so the best targets are rotationally symmetrical, such as impact craters, certain types of lava domes, and

small cinder cones. Features such as barchan dunes and ice flows lack rotational symmetry, however, these dunes may be identified by rotating the barchan template. Diamond Eye can be used to detect the distinct umbrella-shaped volcanic plumes that emanate on Io, best detected in limb observations, as well as the circular and oval plume deposits on Io's surface. The amazing streaked-out cryo-volcanic plumes of Triton (see Figure 10) have morphological terrestrial analogues in the form of volcanic plumes and smoke from forest and oil fires.

4.8 ASC Static target observations

4.8.1 Hypsometry

Hypsometric analysis measures the distribution of ground-surface area with respect to elevation. It has long been employed to study planet-wide distributions of elevation [*Rosenblatt et al., 1994*]. However, a relatively simple procedure can be used for local topography, employing algorithms that detect anomalies or subtle changes. The procedure was applied to Magellan Mission radar altimetry data for Venus by Finn et al. (1995).

The hypsometric procedure selects isolines (horizontal planes of equal elevation) and determines their intersection at various altitudes represented in the altimetry data. The isoline spacing is based on stability with regard to altitude variations. The intersections with topography can be thought of as a multi-mode histogram of frequency (number of intersection points) versus elevation. The map pattern of each histogram mode can then be analyzed to see if it forms a geometric pattern (quasi-circular, linear, etc.), which would have structural or tectonic significance. The detailed analysis of immense data sets can be performed in this way with selections made of identified anomalies for actual transmission to be followed by further analysis.

4.8.2 Interferometry

Radar interferometry is a powerful analytical technique capable of detecting feature deformation, for example, volcano deformation caused by changes in internal pressure due to magma movement. Although interferometry is outside the purview of the ASC autonomous science analysis mission, it will be possible to carry out a demonstration of the technique on returned data. Generally, volcanoes inflate prior to eruption and magma moves towards the surface, and deflate post-eruption. The scale of deformation is on scales ranging from centimeters to decimeters over tens of square kilometers. Interferometry relies on observations being made at the same incidence angle, polarization, and pulse bandwidth, criteria which are matched by ASC. To show change, both before and after images must exist. However, the large amount of processing necessary to produce interferograms and the low cross-spacecraft data transferal rate (~160 Kb/sec) means that widespread autonomous interferometry is not possible onboard ASC. However, we may include interferometric analysis of a selected target, and this can be expanded in high-priority cases where "before" imagery exists. Certainly, interferometric analyses will be performed on suitable data returned to ground.

As an example of a target case, we intend to study selected volcanoes on Isla Isabela and Isla Fernandia in the western Galapagos Islands. These islands, made up of six volcanoes (Figure 22) demonstrated both inflation (often an eruption precursor) and deflation in interferograms generated from ERS-1 and ERS-2 data obtained in 1992 and 1997, and 1992 and 1998 (Amelung et al., 2000). The largest volcano on Isla Isabela, Sierra Negra, has not recently erupted, but undergoes periodic

inflation and deflation. ASC therefore has the opportunity to continue monitoring this interesting location, increasing temporal coverage of the volcanic processes.

ASC also has the potential to revisit previously targeted sites if a large amount of change occurs (if a volcano erupts, or if warning is received of pending or current activity at a given location). The target can then be monitored for later determination of change in shape. In the case of large earthquakes, ASC has potentially two roles: the first is the detection of small-scale change (such as surface ruptures, ground collapse and landslides) detectable by the change-detection software. The second consists of regional change detectable from interferometric analysis of returned data, so long as suitable data for comparison exists.

5.0 Onboard operations

5.1 Automatic operation replanning and resource useage

Traditionally, spacecraft have been controlled through linear (non-branching) command sequences that have been carefully designed on the ground. Recently, automated planning systems have been used in ground operations to enable significant automation. Ground-based automated planning for the DATA-CHASER shuttle payload in 1997 enables an 80% reduction in command generation effort and a 40% increase in science return compared to manual commanding [Chien et al., 1999; Rabideau et al. 1999]. Use of ASPEN planning system for the Modified Antarctic Mapping Mission (MAMM) in the Fall of 2000 [Smith et al. 2001] enabled development of the data acquisition plan in weeks whereas acquisition plan development for the 1997 AMM-1 mission took 1 year.

While reducing the amount of time and effort in ground-based production of mission operations plans can enable significant mission improvement onboard deployment of the planning system offers even more payoff. Because uplink and downlink contacts are infrequent, and round trip light times for deep space missions can be significant, even fully automated ground-based planning is limited in its response time to anomalies, science opportunities, and other execution feedback.

As a counterpoint, enabling significant onboard decision-making is a significant departure from how space missions are currently flown. Onboard autonomy requires a significant change in mindset for both mission operations and science teams. Flying onboard planning as a New Millennium Experiment over the extended duration of the Techsat-21 mission will enable future missions to leverage this high payoff technology.

We will fly the Continuous Activity Scheduling Planning Execution and Replanning (CASPER) planning system [Chien et al 1999, 2000] as the onboard planning component of our Autonomous Sciencecraft Constellation experiment. From a research perspective this is a mature piece of software, and is being used in a number of research prototypes for Deep Space Communications Station Control [Fisher et al. 1999], onboard rover planning [Estlin et al. 1999], constellation management, and spacecraft control.

5.2 Onboard data co-registration

In order to carry out accurate autonomous change detection it is necessary to have precise co-registration of images. With highly accurate pointing of the spacecraft possible using interferometric GPS, it is expected that first-order onboard co-registration of images, using on-

board position data will be sufficient to produce co-registration to within 10 m (10 pixels) or better. In areas where open expanses of newly uncovered water or lava flows or lahars have been emplaced, where there is a significant difference between the backscattering on the new unit compared to the unchanging background (e.g., water v. ice, or lava v. vegetation) a simple histogram of pixel counts of backscattering coefficients will suffice to determine areas of change.

5.3 Onboard data processing

The onboard science software will be responsible for forming (possible reduced resolution) SAR imagery onboard and performing feature extraction to drive subsequent science activities. In this section the SAR image construction process is described. We then describe the families of feature extraction algorithms and also show that they will fit within processing requirements and drive the science decisions described above in Science Mission Concept.

The first processing step is to form the SAR image onboard. For an approximately 15 km diameter circular SAR image from a single spacecraft returns first approximation calculations are that such an image is 1.4GB storage or 177M pixels (each pixel is 4 bytes I (real) plus 4 bytes Q (imaginary)). Standard beam-formation algorithms are baselined at 2Kops/pixel, resulting in 10.5K seconds (190 minutes) to form the image on the Techsat-21 payload processor. If this processing is too expensive the resolution can be halved to approximately ¼ the processing time (the algorithms are $2n^2 \log(n)$), or the area observed reduced while maintaining resolution. This would result in image formation in less than 50 minutes, considerable less than the 90 minute orbit decision cycle for downlink, and shows that image formation time fits within reasonable payload processor constraints.

The processed SAR image can then be used to measure ground characteristics. Specifically, for the change detection experiments described above, fresh lava and old, weathered lava have very different backscatter properties and thus new lava flows can be easily detected. Likewise, for flood detection water has different backscatter characteristics from soil, and for ice melt detection ice has different backscatter characteristics from soil or water. For all of the above scenarios change detection algorithms can determine areas of change between two SAR images using a simple order n^2 algorithm.

5.4 Data storage

The total ASC hard drive capacity is 160 GB, of which 40 GB are allocated to data. However, for purposes of autonomous science operations, it is necessary to store either images or a representation of those images (e.g., boundary locations) on-board so new data have a baseline for comparison. Each pixel of an image requires 8 bytes of storage. An image covering 100 km^2 therefore requires 0.8 GB of storage at 1 m resolution: a 9.6 GB worth of data therefore covers 1200 km^2. A typical ASC radar footprint covers 3 x 3 km: assuming 1 m resolution, and produces a dataset of size 72 Mb. At three meter resolution, the dataset is 8 Mb. The three ASC satellites can be used together to form an image from adjacent swathes. Additionally, retargeting of individual satellites on the same pass can be accomplished in microseconds in delta angles are small, as is the case to obtain adjacent swathes. This allows a target of size 10-50 km across to be imaged.

5.5 Downlink

As much science data as possible will be returned during the ASC mission. Individual images can be very large: a single radar image may be up to 9.6 GB, which would take four days to download. Most ASC radar products will be considerably smaller than this, typically of size 80 MB.

On occasion it may be desirable to download large images if the science content is deemed to be high enough, and for verification of the results produced by the onboard science processing algorithms.

5.6 Mission strategy and timeline

The ASC mission is scheduled to be launched in July 2004, with a provisional mission length of 1 year. If the first year is successful, then an extension for a second year is likely. This will greatly enhance the ability of the science team to study processes that have seasonal variability, such as the formation and breakup of ice on lakes.

During the first year of the mission, approximately 2.5 months of ASC time is allocated to the science mission, with one month towards the beginning of the mission, and 1.5 months at a later date. This will entail careful planning to ensure observations of processes that are seasonal are made. During the second year, half the time will be allocated to science. The rest of the flight time will be dedicated to orbital configuration change and testing, and validation of the autonomous operations (command and control) software.

6.0 Data release

Data will be downlinked via commercial stations such as Datalynx or United Space Network. Historically, processing SAR data has required a great deal of computer time on special-purpose computer systems. However, ASC scientists will benefit from onboard processing and identification of important areas undergoing dynamic change, as the data would have been processed prior to downlink. This is a considerable advance over the previous analysis of SAR data. A detailed analysis of the ASC-derived products will take another nine months from receipt time. Data will be exchanged to meet the needs of the science investigators. AFRL offices of public relations will release selected images to the press during the mission. Mission press conferences may also take place at ASU and U. Arizona. All data will be calibrated and processed at AFRL and/or other locations connected via the internet, before electronic transfer to the mission teams. For events that could pose public hazards, such as large volcanic eruptions or floods, selected information and analysis could be released immediately to the appropriate public safety agencies. All appropriate data will be released within one year of receipt. The data will be archived at AFRL.

7.0 Educational Outreach

An Educational and Public Outreach proposal is in development. Educational Outreach activities associated with the ASC mission include an informative website, press releases and public addresses, and the development of bilingual educational activities demonstrating change detection and the benefits of autonomous activity with separate activities for different grade levels. Another possibility under discussion is an educational competition among high schools for proposals of areas they want to image and study. Alternatively, schools could create their own targets to be imaged by ASC to test feature recognition and change detection, and then apply what is learned to an extraterrestrial site.

Websites of interest.

Autonomous Sciencecraft Constellation (ASC)
http://ASC

New Millennium Program
http://nmp.jpl.nasa.gov/index_flash.html

The NASA Solar System Enterprise (SSE) roadmap is available at
http://sse.jpl.nasa.gov/roadmap/pdffiles/Rmap.pdf

NASA/JPL Synthetic Aperture Radar home page
http://southport.jpl.nasa.gov

Shuttle imaging radar (SIR-C/X-SAR)
http://www.jpl.nasa.gov/radar/sircxsar/

Shuttle Radar Topography Mission (SRTM)
http://www.jpl.nasa.gov/srtm

Jet Propulsion Laboratory
http://jpl.nasa.gov

JPL Diamond Eye
www-aig.jpl.nasa.gov/public/mls/diamond_eye/body.htm

Air Force Research Laboratory
www.afrl.af.mil

University of Arizona, Dept. Hydrology and Water resources
www.hwr.arizona.edu/deptinfo.html

Arizona State University, Dept. of Geological Sciences
geology.asu.edu/research/planetary/planetary.html

NASA Earth Science Enterprise Natural Hazards
ltpwww.gsfc.nasa.gov/senh/nathaz.htm

Smithsonian Institute Global Volcanology Project
www.volcano.si.edu/gvp/volcano/index.htm

US Geological Survey Decade Volcanoes
vulcan.wr.usgs.gov/Volcano/Decade/Volcanoes/DecadeVolcanoes/framework.html

8.0 References.

Amelung, F., S. Jonsson, H. Zebker and P. Segall, Widespread uplift and 'trapdoor' faulting on Galapagos volcanoes observed with radar interferometry, *Nature*, 407, 993-996, 2000.

Baker, V.R., Water and the Martian landscape, *Nature*, 412, p. 228-236, 2001.

Baker, V. R., and D. J. Milton, Erosion by catastrophic floods on Mars and Earth, *Icarus*, 23, 27-41, 1974.

Baker, V.R., The Spokane Flood controversy and the Martian outflow channels, *Science*, 202, 1249-1256, 1978.

Baker, V. R., R. G. Strom, V. C. Gulick, J. S. Kargel, G. Komatsu, and V. S. Kale, Ancient oceans, ice sheets and the hydrological cycle on Mars, *Nature*, 352, 589-594, 1991.

Baker, V. R., R. G. Strom, J. M. Dohm, V. C. Gulick, J. S. Kargel, G. Komatsu, G. G. Ori, and J. W. Jr. Rice, Mars' Oceanus Borealis, ancient glaciers, and the MEGAOUTFLO hypothesis, *Lunar Planet. Sci. Conf.* [CD-ROM], XXXI, abstract 1863, 2000.

Brackenridge, G. R., J. C. Knox, E. D. Paylor, and F. J. Magilligan, Radar remote sensing aids study of the great flood of 1993, EOS, 75, 521-527, 1994.

Breed, C. S., M. J. Grolier and J. F. McCauley, Morphology and Distribution of common "sand" dunes on Mars: comparison with the Earth. *J. Geophys. Res.*, 84, 8183-8204, 1979.

Burl, M. C., L. Asker, P. Smyth, U. Fayyad, P. Percona, J. Aubele and L. Crumpler. Learning to recognize volcanoes on Venus, Machine Learning, 30, 165-195, 1998.

Burl, M. C., C. Fowlkes and J. Roden. Mining for image content, In, Systemics, Cybernetics, and Infomatics / Information Systems , Analysis and Synthesis, Orlando, Florida, July 1999.

Burl, M. C., C. Fowlkes, J. Roden, A. Stechert and S. Mukhtar. Diamond Eye: A distributed architecture for image data mining, In, SPIE AeroSense Conference on Data Mining and Knowledge Discovery, Orlando, Florida, July 1999.

Burr, D.M., McEwen, A.S., and Sakimoto, S.E.H., Recent aqueous floods from the Creberus Rupes, Mars. Geophys. Re. Lett., submitted.

Chien, S., G. Rabideau, J. Willis, T. Mann, "Automating Planning and Scheduling of Shuttle Payload Operations," *Artificial Intelligence Journal,* 1999.

Chien, S., R. Knight, A. Stechert, R. Sherwood, and G. Rabideau, "Using Iterative Repair to Improve Responsiveness of Planning and Scheduling," *Proceedings of the Fifth International Conference on Artificial Intelligence Planning and Scheduling*, Breckenridge, CO. April, 2000.

Davies, A. G., R. Lopes-Gautier, W. D. Smythe and R.W. Carlson. Silicate cooling model fits to Galileo NIMS data of volcanism on Io, *Icarus,* 148, 212-225, 2000.

Davies, A. G., L. P. Keszthelyi, D. Williams, C. B. Phillips, A. S. McEwen, R. M. C. Lopes, W. D. Smythe, L. W. Kamp, L. A. Soderblom and R. W. Carlson. Thermal signature, eruption style and eruption evolution at Pele and Pillan on Io. *J. Geophys. Res.*, in press, 2001.

Davies, A. G., Volcanism on Io: estimation of eruption parameters from Galileo NIMS data. Submitted to *J. Geophys. Res.-Planets.*

Dohm, J. M., R. C. Anderson, V. R. Baker, J. C. Ferris, T. M. Hare, R. G. Strom, L. P. Rudd, J. W. Jr. Rice, and D. H. Scott, System of gigantic valleys northwest of Tharsis Montes, Mars: Latent catastrophic flooding, northwest watershed, and implications for northern plains ocean, *Geophys. Res. Lett.*, 27, 3559-3562, 2000a.

Dohm, J.M., R. C. Anderson, V. R. Baker, R. G. Strom, R.G., G. Komatsu, and T. M. Hare, Pulses of magmatic activity through time: Potential triggers for climatic variations on Mars, *in* Lunar and Planetary Science XXXI: Lunar and Planetary Institute, Houston, Texas, Abstract No. 1632, 2000b.

Edgett, K. S., M. C. Malin, R. J. Sullivan, P. Thomas, and J. Veverka, Dynamic Mars: new dark slope streaks observed on annual and decadal time scales, *Lunar Planet. Sci. Conf.* [CD-ROM], XXXI, abstract 1058, 2000.

Estlin T., J. Yen, R. Petras, D. Mutz, R. Castano, G. Rabideau, R. Steele, A. Jain, E. Mjolsness, A. Gray, T. Mann, S. Hayati and H. Das, An integrated architecture for co-operating rovers. Proc. 5th International Symposium on Artificial Intelligence and Automation in Space, iSAIRIS-99, Noordwijk, the Netherlands, 1999.

Finn, V., V. R. Baker, A. Z. Dolginov, I. Gabitov, and A. Dyachenko, Large-scale spatial patterns in topography at Alpha Regio, Venus, *Geophys. Res. Lett.*, 22, 1901-1904, 1995.

Giacomelli, A., M. Mancini, and R. Rosso, Integration of ERS-1 PRI imagery and digital terrain models for the assessment of flooded areas, earthnet online, esa, 1998.

Gwinner, K., E.Hauber, R. Jaumann, and G. Neukum, High-resolution, digital photogrammetric mapping: a tool for earth science, EOS, 81 (44), 2000.

Hirschboeck, K. K., Catastrophic flooding and atmospheric circulation anomalies, *in* Catastrophic flooding, L. Mayer and D. B. Nash, editors, Allen & Unwin, p. 23-56, 1987.

Hirschboeck, K. K., Climate and floods, U. S. Geological Survey Water-supply Paper, 2375, 1991.

Kargel, J. S., V. R. Baker, J. E. Beget, J. F. Lockwood, T. L. Pewe, J. S. Shaw, and R. G. Strom, Evidence of ancient continental glaciation in the Martian northern plains, *J. Geophys. Res.*, 100, 5351-5368, 1995.

Keszthelyi, L.P., A. S. McEwen, C.B. Phillips, M. Milazzo, P. Geissler, D. Williams, E. Turtle, J. Radebaugh, D. Simonelli and the Galileo SSI Team, Imaging of volcanic activity on Jupiter's moon Io by Galileo during GEM and GMM, *J. Geophys. Res.*, in press, 2001.

Jöns, H. P., Arcuate ground undulations, gelifluxion-like features and "front tori" in the northern lowlands on Mars, what do they indicate?, (abstract), *Lunar. Planet. Sci. Conf.*, XVII, 404-405, 1986.

Laugier, O., Fellah, K., Tholey, N., Meyer, c., and de Fraipont, P., High temporal detection and monitoring of flood zone dynamic using ERS data around catastrophic natural evetns: the 1993 and 1994 Camargue, earthnet online, esa, 1998.

Leconte, R. and D. Klassen. Lake and river ice investigations in northern Manitoba using airborne SAR imagery, *Arctic*, 44, 153-163, 1991.

Lucchitta, B. K., H. M. Ferguson, and C. Summers, Sedimentary deposits in the northern lowland plains, Mars, *J. Geophys. Res.*, 91, E166-E174, 1986.

Malin, M.C., and Edgett, K.S., Evidence for recent groundwater seepage and surface runoff on Mars, Science 288, 2330-2335, 2000.

McEwen, A.S., M.J.S. Belton, H.H. Breneman, S.A. Fagents, P. Geissler, R. Greeley, J.W. Head, G. Hoppa, W.L. Yaeger, T.V. Johnson, L. Keszthelyi, K.P. Klassen, R. Lopes-Gautier, K.P. McGee, M.P. Milazzo, J.M. Moore, R.T. Pappalardo, C.B. Phillips, J. Radebaugh, G. Schubert, P. Schuster, D.P. Simonelli, R. Sullivan, P.C. Thomas, E.P. Turtle and D.A. Williams, Galileo at Io: results from high-resolution imaging, *Science, 288,* 1193-1198, 2000.

McEwen, A.S., L. Keszthelyi, J.R. Spencer, D.L. Matson, R. Lopes-Gautier, K.P. Klassen, T.V. Johnson, J.W. Head, P. Geissler, S. Fagents, A.G. Davies, M.H. Carr, H.H. Breneman and M.J.S. Belton, Very high-temperature volcanism on Jupiter's moon Io, *Science, 281,* 87-90, 1998.

Mouginis-Mark, P.J., Recent water release in the Tharsis region of Mars, Icarus 84, 362-373

McCauley, J.F., G.G. Schaber, C.S. Breed, M.J. Grolier, C.V. Haynes, B. Issawi, C. Elachi, and R.G. Blom, Subsurface valleys and geoarchaeology of eastern Sahara revealed by shuttle radar, *Science*, 218, 1004-1019, 1982.

Pappalardo, R.T., M.J.S. Belton, H.H. Breneman, M.H. Carr, C.R. Chapman, G.C. Collins, T. Denk, S. Fagents, P.E. Geissler, B. Giese, R. Greeley, R. Greenberg, J.W. Head, P. Helfenstein, G. Hoppa, S.D. Kadel, K.P. Klaasen, J.E. Klemaszewski, K. Magee, A.S. McEwen, J.M. Moore, W.B. Moore, G. Neukum, C.B. Phillips, L.M. Prockter, G. Schubert, D.A. Senske, R.J. Sullivan, B.R. Tufts, E.P. Turtle, R. Wagner, and K.K. Williams, 1999, Does Europa have a subsurface ocean? Evaluation of the geological evidence, *J. Geophys. Res.*, 104, 24,015-24,055.

Parker, T. J., D. M. Schneeberger, D. C. Pieri, and R. S. Saunders, Geomorphic evidence for ancient seas on Mars, in *Symposium on Mars: Evolution of its Climate and Atmosphere, LPI Tech. Rept. 87-01*, 96-98, 1987.

Rabideau, G., R. Knight, S. Chien, A. Fukunaga, A. Govindjee, "Iterative Repair Planning for Spacecraft Operations in the ASPEN System," *International Symposium on Artificial Intelligence Robotics and Automation in Space (ISAIRAS),* Noordwijk, The Netherlands, June 1999.

Rao, D.P., V. Bhanumurthy, G.S. Rao, and P. Manjusri, Remote sensing and GIS in flood management in India, in *Flood Studies in India*, edited by V.S. Kale, pp. 195-218, Geological Society of India, Bangalore, 1998.

Rosenblatt, P., P. C. Pinet, and E. Thouvenot, Comparative hypsometric analysis of Earth and Venus, *Geophys. Res. Lett.*, 21, 465-468, 1994.

Scott, D. H., J. M. Dohm, and J. W. Jr. Rice, Map of Mars showing channels and possible paleolake basins, *USGS Misc. Inv. Ser. Map I-2461 (1:30,000,000)*, 1995.

Simkin, T. and L. Seibert, "Earth's volcanoes and eruptions: an overview," in *Encyclopedia of volcanoes*, eds. H. Sigurdsson, Academic Press, pp 249-262, 1999.

Smith, B., B. Engelhardt, D. Mutz, J. Crawford, 2001, "Automating the Mission Planning for the Second Antarctic Mapping Mission," *Proceedings of the 4th International Symposium on Reducing the Cost of Spacecraft Ground Systems and Operations.*

Smith, L. C., 1997, Satellite remote sensing of river inundation area, stage, and discharge: A review, Hydrological Processes, 11, 1427-1439.

Sullivan, R., M. Malin, and K. Edgett, Mass-Movement Slope Streaks Imaged by the Mars Orbital Camera, *JGR Planets*, in press.

Finn, V., V. R. Baker, A. Z. Dolginov, I. Gabitov, and A. Dyachenko, Large-scale spatial patterns in topography at Alpha Regio, Venus, *Geophys. Res. Lett.*, 22, 1901-1904, 1995.

Swift, C.T., W.L. Jones, R.F. Harrington, J.C. Fedors, R.H. Couch, and B.L. Jackson, Microwave radar and radiometric remote sensing measurements of lake ice, *Geophys. Res. Lett.*, 7, 243-246, 1980.

Tsoar, H., R. Greeley and A. H. Peterfreund, Mars: the North Polar sand sea and related wind patterns, *J. Geophys. Res.*, 84, 8167-8180, 1979.

Williams, G.P., 1965. Correlating Freeze-up and Break-up with Weather Conditions, *Canadian Geotechnical Journal*, 2, 313-326.

Williams, G.P., A Note on the Break-up of Lakes and Rivers as indicators of Climate Change, *Atmosphere*, 8, 23-24, 1970.

Zebker, H. A., P. A. Rosen, S. Hensley and P. Mouginis-Mark, Analysis of active lava flows on Kilauea volcano, Hawai'i, using SIR-C radar correlation measurements, *Geology*, 24, 495-468, 1996.

9.0 ASC Science Team

Ashley Davies is the Science Lead for the Autonomous Sciencecraft Constellation. Ashley is a Research Scientist at the Jet Propulsion Laboratory, California Institute of Technology, and is a member of the Galileo Near Infrared Mapping Spectrometer Team. He has a Bachelor of Science degree in astronomy and geology from the University of Hertfordshire (UK) and a Doctorate in planetary volcanism from Lancaster University (UK). His main fields of interest are all aspects of planetary volcanism (especially volcanic thermal emission, eruption dynamics, and flow emplacement mechanisms) the jovian satellite Io, and developing autonomous geological analysis techniques to automate the science discovery process. Ashley is currently working on in-situ measurements of volcanic thermal emission in order to better understand remotely-sensed terrestrial and extraterrestrial datasets. Ashley has extensive field experience in Northern Scotland, and the Hawaiian Islands. He is a co-investigator on a proposed Discovery-class mission (Argus) to monitor volcanism on Io, and OMEGA, a mission proposed under New Millennium Program-ST7, that will autonomously detect and model volcanic thermal emission from Earth orbit.

Ronald Greeley has been involved in lunar and planetary studies since 1967. Current research is focused on gaining an understanding of planetary surface processes and geological histories. The approach involves a combination of spacecraft data analysis, laboratory experiments, and geological field studies on Earth of features analogous to those observed on the planets. Prof. Greeley has worked on Mars Pathfinder, Galileo-Jupiter project, NASA Mars Polar Lander and Mars Express, as well as determining Mars landing sites for exobiology, geological mapping of Venus, the Astrobiology Institute, and the Shuttle Radar Laboratory. His field studies include aeolian and volcanic terrains. Greeley has served on various National Academy of Science committees dealing with planetary science, including a panel to assess the major directions for Space Science in the period 1995-2015. He currently serves on several NASA committees. Author or co-author of 10 books and more than 100 papers, Greeley also serves on editorial panels for several journals and is Associate Editor for the Planetary Science Series of Cambridge University Press.

Kevin Williams is a member of the ASC Science Team and is a Ph.D. candidate in planetary geology and remote sensing at Arizona State University. He received a Bachelor of Arts degree in astronomy and physics from Boston University and a Master of Arts degree in planetary geophysics from Johns Hopkins University. Kevin's dissertation research involves laboratory measurements of radar signal attenuation by sand and dust with image analysis and field studies in a dune field in the Mojave Desert. These results have implications for the design of future radar imaging missions for the study of Earth and Mars. Other research interests include radar imaging of geologic features, impact cratering, tectonic processes on Europa, and the comparative geologic history of the terrestrial planets.

Victor R. Baker is Regents Professor, and Chair of the Department of Hydrology and Water Resources at the University of Arizona. Prof. Baker has nearly three decades experience with Mars geomorphology and paleohydrology, fluvial sedimentology, glacial and quaternary geology, the geology of natural hazards, and the geomorphology of planetary surfaces. He is an expert on fluvial geomorphology and paleohydrology research, and has published extensively on geological reasoning and modes of inference. He has extensive field experience throughout the Western United States and Australia.

James Dohm is a senior researcher at the University of Arizona. He works with Vic Baker on geological investigations that document geologic processes at local, regional, and global scales for Earth, Mars, and Venus (e.g., including magmatic-driven activity and catastrophic flooding). Mr. Dohm has extensive field experience coupled with more than 13 years of experience with Mars-related geological research, which includes publishing 6 USGS I-maps at four map scales, and twelve years as assistant coordinator to the NASA-based Planetary Mapping Program. His terrestrial mapping experience includes investigations of the volcanic and tectonic histories Mormon and San Francisco volcanic fields, Northern Arizona.

Appendix 1: Change detection target lists and descriptions

Figure 11 shows the locations of targets within the baseline 28.5 degrees latitude constraint imposed by the ASC orbit, as well as the latitude limits for an orbit of 40 degrees inclination. Targets include volcanoes, dune fields and ice formation/retreat sites. Sites outside of the continental United States are shown. Sample ground tracks are also shown. Target types are discussed below.

A1.1 Ice features

Table A1 shows potential ice-process targets where the seasonal formation and breakup of ice can be detected and then monitored.

Table A1.1: Ice-related targets

Latitude	Longitude	Target	Country	Process
34.86 N	79.7 E	Lake	India	Ice Fm.
33.06 N	77.9 E	Lake	India	Ice Fm.
29.94 N	85.33 E	Lake	China	Ice Fm.
29.94 N	85.3 E	Lake	China	Ice Fm.
30.56 N	86.03 E	Lake	China	Ice Fm.
34 N	80.74 E	Lake	China	Ice Fm.
34.39 N	80 E	Lake	China	Ice Fm.
34.43 N	80.05 E	Lake	China	Ice Fm.
33.7 N	78.47 E	Lake	Kashmir	Ice Fm.
16.18 S	68.61 W	Lake	Bolivia	Ice Fm.
16.15 S	68.59 W	Lake	Bolivia	Ice Fm
16.86 S	69.05 W	Lake	Bolivia/Peru	Ice Fm.

A1.2 Volcanic features

Table A1.2 shows an initial list of volcanoes within the observable parameters of the orbit of ASC, from which a final selection will be made. Not including hypsometry, there are three types of volcano observation listed in Table A1.2. Consistently active volcanoes, where there is an extremely high probability of change detection, are part of the base science mission. Decade volcanoes are volcanoes that may not necessarily show change during the mission, but which will be closely monitored for signs of volcanic activity and are low-probability but high priority targets. The third type ("Other Targets") are also volcanoes where detection of change is likely over the lifetime of the ASC mission and which have varying priority, to be imaged in the event of activity or predictions of activity.

Table A1.2. Potential ASC volcano target list				
Volcano	Volcano type	latitude	Longitude	summit elevation, m
Consistently active				
Arenal, Costa Rica,	stv	10.463 N	84.703 W	1657
Bagana, Bourganville Island	lc	6.14 S	155.19 E	1750
Dukono, Halmahera, Indonesia	cx	1.70 N	127.87 E	1185
Erta Ale, Ethiopia	shv, ll	13.60 N	40.67 W	613
Kilauea, Hawaii, US	shv	19.425 N	155.292 W	1222
Langila, New Britain	cx	5.53 S	148.42 E	1330
Manam, Papua, New Guinea	stv	4.10 S	145.06 E	1807
Pacaya, Guatemala	cx	14.38 N	90.60 W	2552
Sangay, Equador	stv	2.03 S	78.34 W	5188
Santa Maria, Guatemala[1]	stv	14.756 N	91.552 W	3772
Semeru, Java	stv	8.11 N	112.92 E	3676
Decade volcanoes				
Colima, Mexico	sv (2001)[2]	19.514 N	103.62 W	3850
Galeras, Colombia	cx (2000)	1.22 N	77.37 W	4276
Mauna Loa, Hawai'i, US	shv (1984)	19.475 N	155.608 W	4170
Merapi, Java, Indonesia	stv (2001)	07.54 S	110.44 E	2911
Nyiragongo, Zaire	stv, ll? (1995)	1.52 N	29.25 E	3469
Taal, Luzon, Phillipines	stv (1977)	14.002 N	120.993 E	400
Teide, Canery Islands, Spain	stv (1909)	28.3N	16.6W	3715
Ulawun, Papua, New Guinea	stv (2000)	5.04 S	151.34 E	2334
Unzen, Kyushu, Japan	cx (1996)	32.75 N	130.30 E	1500
Other targets				
Etna, Sicily, Italy	stv (2001)	37.73 N	15.00 E	3315
Pinatubo, Luzon, Philippines	stv (1996)[3]	15.13 N	120.35 E	1486
Popocatepetl, Mexico	stv (2000)	19.023 N	98.622 W	5426
Sakura Jima, Kyushu, Japan	stv (2000)	31.58 N	130.67 E	1117
San Cristobal, Galapagos Is. Islands	stv (2000)[4]	12.702 N	87.004 W	1745
Soufriere Hills, Montserrat, West Indies	stv (2001)	16.72 N	62.18 W	915

notes:

1 Santa Maria is also a Decade volcano.

2 Year of last eruption in brackets.

3 Lahar. Pinatubo erupted in 1991.

4 Devastating lahar caused by Hurricane Mitch in 1998.

key to abbreviations.

lc lava cone
ll lava lake
cx complex volcano
shv shield volcano
stv stratovolcano

A1.3 Aeolian features

Potential Aeolian Targets are shown in Table A1.3.

Table A1.3 Potential Aeolian Targets

Latitude	Longitude	Target	Country	Process
Sand dunes				
19.1 N	19.5 E	Dunes	Chad	Migration
25.5 N	30.5 E	Dunes	Egypt	Migration
25.75 N	30.5 E	Dunes	Egypt	Migration
24.95 N	30.6 E	Dunes	Egypt	Migration
22 N	30.6 E	Dunes	Sudan	Migration
18.36 N	19.9 N	Dunes	Chad	Migration
22.89 S	125.23 E	Dunes	Australia	Migration
Wind streaks				
18.53 S	68.54 W	Streaks	Bolivia	Backscatter
12.83 N	16.33 E	Streaks	Chad	Backscatter
23.17 N	30.83 E	Streaks	Egypt	Backscatter
24.80 N	26.37	Streaks	Egypt	Backscatter
20.34 S	137.3 E	Streaks	Australia	Backscatter
18.84 N	19.31 E	Streaks	Chad	Backscatter
22.94 S	18.4 E	Streaks	Namibia	Backscatter
29.5 N	41.0 E	Streaks	Saudi Arabia	Backscatter
24.27 N	43.39 E	Streaks	Saudi Arabia	Backscatter
33.35 N	37.0 E	Streaks	Syria	Backscatter
31.21 N	21.0 E	Streaks	Libya	Backscatter
31.25 N	65.0 E	Streaks	Afghanistan	Backscatter
33.24 N	46.14 E	Streaks	Iraq	Backscatter
19.5 S	22 E	Streaks	Botswana	Backscatter
Other				
21.84 S	129.6 E	Sand cover	Australia	Penetration

A1.4 Flood features

Floods have occurred in the distant past on Mars, and may occur on Europa and Titan. Floods of a different type (silicate lava and sulphur) are regularly emplaced on Io. On Earth, floods events are strongly dependent on the time of year (season). Examples of locations with greatest probability of detecting "in-situ" flood-related effects include the southern, southeastern, and eastern parts of the United States, northern India, southeastern Africa, central Australia, central South America, and Central America. In India, for example, the optimal viewing period is during the monsoon season (from June to November), a period of high rainfall. Additional targets for ASC with easily-verifiable ground truth are dry lake beds in Southern California: at Goldstone Lake, Searles Lake, Rogers Lake, Coyote Lake, Lucerne Lake, and Panamint Flat.

Table A1.4: Flood Process Target List (examples)

Location	Latitude and longitude	Time of year	Process type
Bangladesh (Ganges)	23.0 N, 89.8 E	Monsoon (July)	River flood
Guangxi, S.E. China	23.0 N, 112.0 E	Winter	River flood
Manaus, Brazil	3.5 S, 59.0 W	Summer	River flood
Goldstone Lake, CA.	35.4 N, 116.9 N	Winter	Dry lake bed filling
Panamint Lake, CA.	36.1 N, 117.3 W	Winter	Dry lake bed filling
Coyote Lake, CA.	35.1 N, 116.8 W	Winter	Dry lake bed filling

A1.5 Planform and other targets.

Potential targets for detection of planform change include all of the volcanoes mentioned above and other sites that are prone to planform change through slippage and deformation.

As part of the base mission, one possible experiment, which will enable calibration and testing of ASC science processing algorithms, revolves around observing created targets of known areal patterns and radar backscattering coefficients. As part of the ASC Education and Public Outreach program, a project by which schools create targets for ASC to detect is being considered. These targets allow change detection and feature detection software to be tested. Other targets that will be suitable for this experiment include irrigated crop circles in desert locations, and playa lakes that seasonally flood.

Table A1.5: Planform and other targets
Volcanoes in list A1.2
Areas prone to landslides
Earthquake-prone areas
Non-process specific targets such as: irrigated crop circles, Saudi Arabia (24 N, 45 E). Scale: 200 to 500 in diameter.

Appendix A2. Diamond Eye Feature Identification Targets

Table A2.2 shows examples of targets suitable for testing the Diamond Eye algorithms.

Table A2.2 Diamond Eye Example Targets		
Location	**Feature**	**Latitude and longitude**
Kilauea, HI	Volcanic cones and craters	19.4 N, 155 W
Mauna Kea, HI	Volcanic cones and calderas	19.8 N, 155.5 W
Mauna Loa, HI	Volcanic craters and calderas	19.47 N, 155.6 W
Meteor Crater, AZ	Impact crater	35 N, 111.5 W
Wolf Creek, W. Aust.	Impact crater	19.3 S, 46 E
Al Kidan, Saudi Arabia	Dunes	22.0 N, 54.5 E
Al Kidan, Saudi Arabia	Dunes	20.7 N, 53.1 E

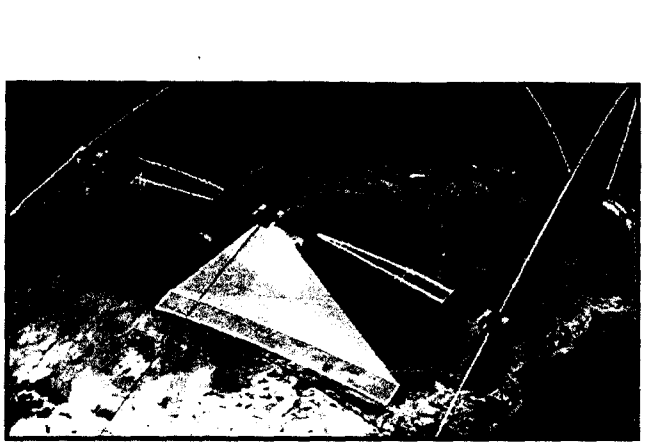

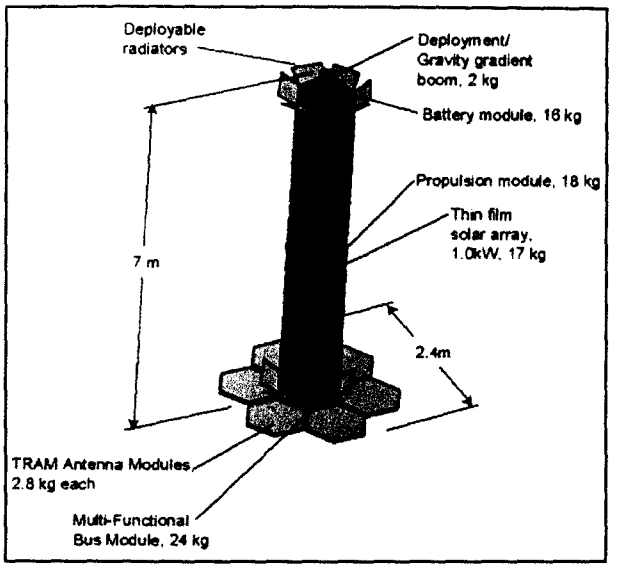

1. Figure 1a (left): The Autonomous Sciencecraft Constellation (ASC) in Earth orbit. The mission will demonstrate autonomous command and control, as well as autonomous data processing to extract scientifically valuable products. Figure 1b (right) shows one of the satellites, each of which is equipped with X-SAR radar.

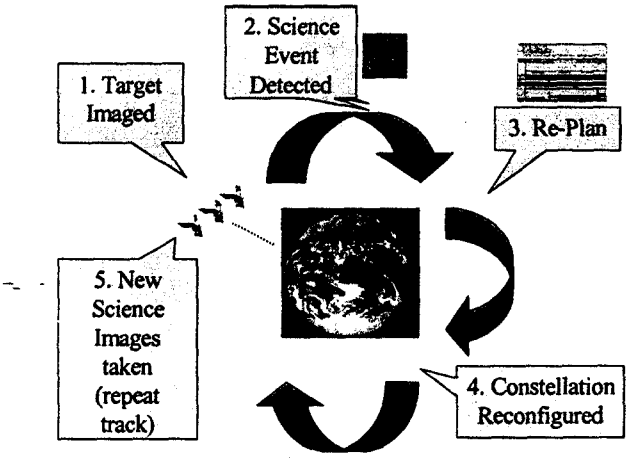

2. ASC science concept, based on the autonomous processing of science data to determine future operations and observations.

3. Dynamic change takes place on the surface of Mars, as evidenced by these streaks, imaged by the Mars Orbiter Camera (MOC) on Mars Global Surveyor (image by Malin Space Science Systems). High-resolution images show seasonal change, the result of freezing and thawing carbon dioxide and water, as well as dune movement and dust devil activity. Such areas where change is occurring are high-priority targets for closer examination.

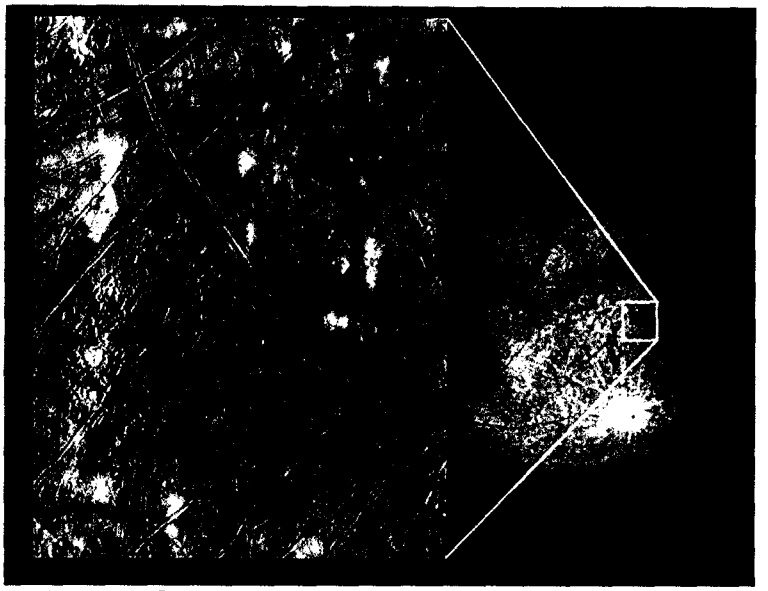

Area of chaos terrain on Europa where blocks of ice are thought to have broken apart and moved into new positions. Areas of chaos appear to be geologically young and would be targets for change detection.

This area of Europa shows evidence of past activity on the icy surface. Mottled terrain, triple bands, cracks, and splotches are all visible in this area. The arrows point to thin, bright linear features which may be the initiation of band or ridge formation. Such features would be targets for change detection on Europa. Image is 400 by 450 km

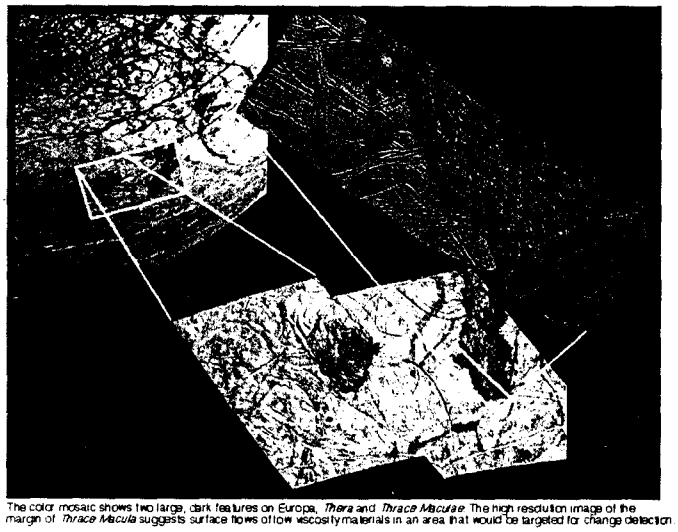

The color mosaic shows two large, dark features on Europa, *Thera* and *Thrace Maculae*. The high resolution image of the margin of *Thrace Macula* suggests surface flows of low viscosity materials in an area that would be targeted for change detection.

4. Figure 4a (top, left) shows an area of chaos terrain on Europa where blocks of ice are thought to have broken apart and moved into new positions. Areas of chaos appear to be geologically young and could be targets for change detection. Figure 4b (lower, left) is a color mosaic showing two large, dark features on Europa, *Thera* and *Thrace Maculae*. The high-resolution image of the margin of *Thrace Macula* suggests surface flows of low viscosity materials in an area that would be targeted for change detection. Figure 4c (right) shows evidence of past activity on the icy surface. Mottled terrain, triple bands, cracks, and splotches are all visible in this area. The arrows point to thin, bright linear features that may be the initiation of band or ridge formation. Such features would be targets for change detection on Europa. Image is 400 by 450 km.

5a Pele (red oval) 5b Pillan (black-eye on Io) 5c

5d Prometheus, !980 (Voyager) 5e Prometheus, 1996 (Galileo)

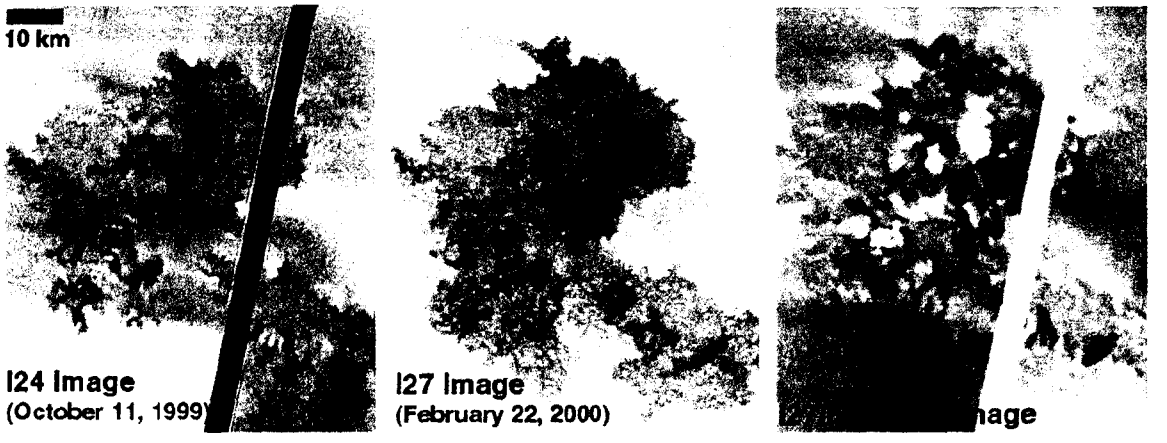

5f 5g 5h (ratio of 5f and 5g)

5. Io is the most volcanically active body in the Solar System: as such, the surface is constantly changing appearance. Changes take place on different spatial and temporal scales. Figure 5a, 5b and 5c show large-scale changes at Pele and Pillan (the black deposit in the middle image, which is 700 km across) over the course of two years of the Galileo mission. Figure 5d and 5e show changes at Prometheus, on a smaller spatial scale and temporal scale (19 years), between the Voyager and Galileo missions. Figure 5f and 5g show the emplacement of relatively small flows (5h) in the course of a few months, at high spatial resolution images.

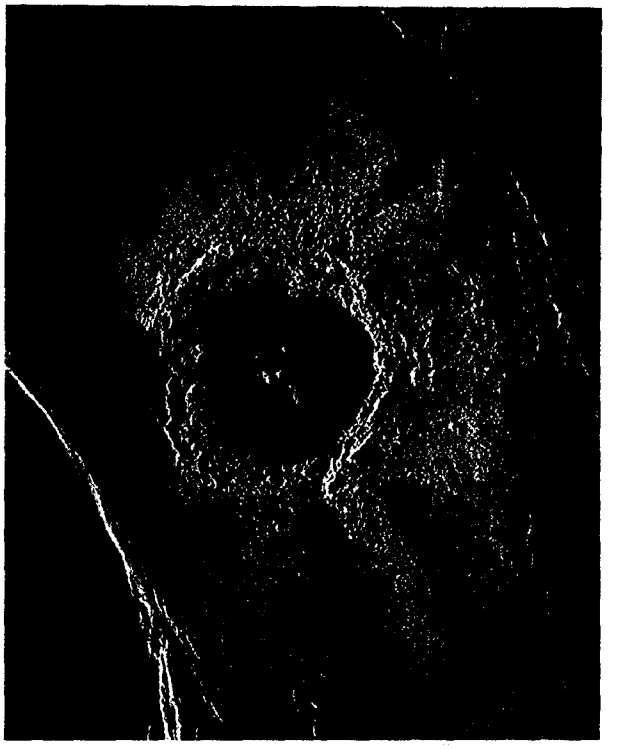

6. The surface of Venus as imaged by Magellan(left). Venus has a very young surface, as evidenced by a low and uniform crater density. It is possible that some areas are still volcanically active. A repeat radar mission would reveal areas of change on the surface, which would be high-priority sites for detailed investigation and sample return.

7. Dickinson Impact Crater (right). This Magellan image is centered at 74.6 degrees north latitude and 177.3 E longitude, in the northeastern Atalanta Region of Venus. The image is approximately 185 kilometers (115 miles) wide at the base and shows Dickinson, an impact crater 69 kilometers (43 miles) in diameter. The crater is complex, characterized by a partial central ring and a floor flooded by radar-dark and radar-bright materials. Extensive radar-bright flows that emanate from the crater's eastern walls may represent large volumes of impact melt, or they may be the result of volcanic material released from the subsurface during the impact event. (NASA P-39716).

8. Robotic explorers throughout the Solar System. Top: Titan Atmosphere Explorer. A vision of the future: a blimp moves through the atmosphere of Titan, dipping down to the surface as necessary to take samples. Such a system would have a high degree of autonomy to cope with sudden environmental changes, and to recognize important scientific targets, as it moves about the satellite. Middle: A Europa Submersible, having drilled through the icy Europan crust, identifies hydrothermal vents, possibly a life-sustaining environment. Such a vehicle would need a high degree of autonomy to operate. Bottom: A Mars sample return mission blasts off from the surface of Mars, observed by an intelligent rover that has identified the rocks of greatest scientific value.

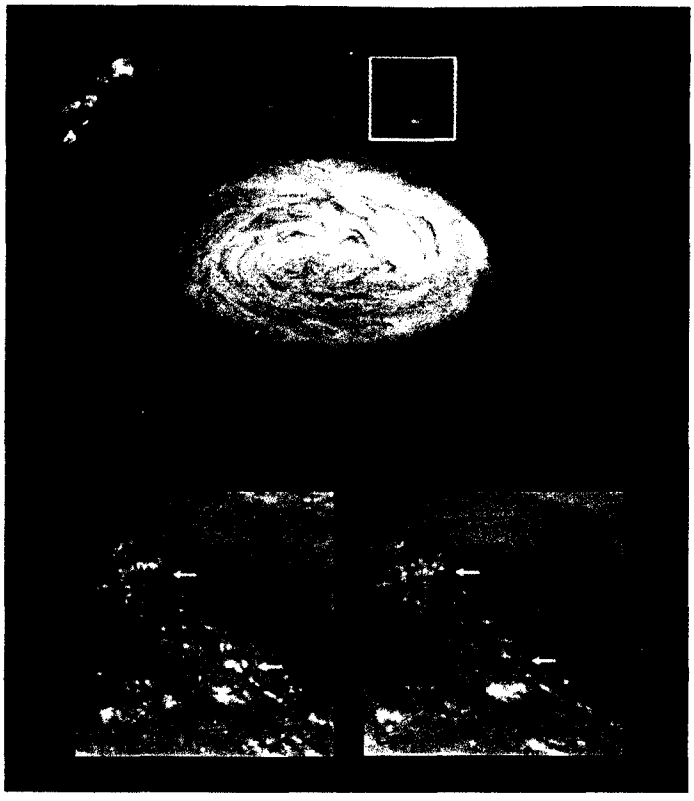

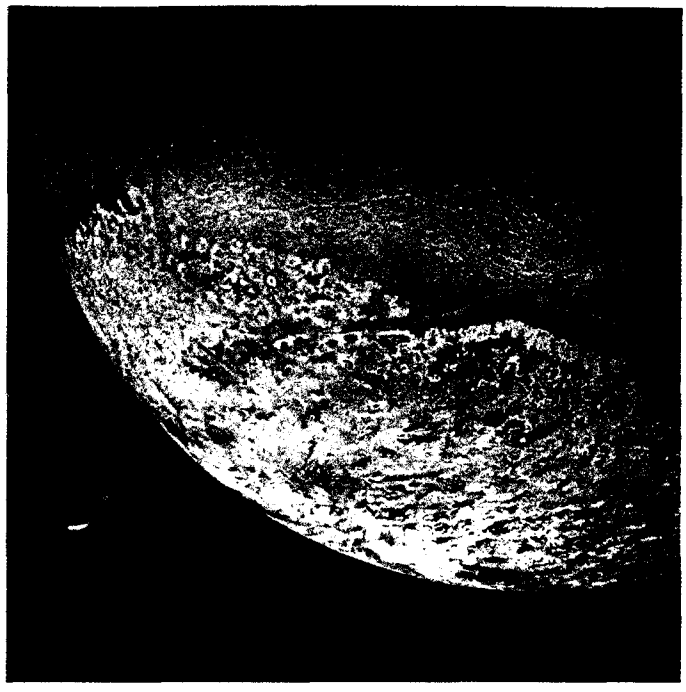

9. (left) Thunderheads on Jupiter bright white cumulus clouds similar to those that bring thunderstorms on Earth - at the outer edges of Jupiter's Great Red Spot. Images from NASA's Galileo spacecraft in June 1996 provided new evidence that thunderstorms may be an important source of energy for Jupiter's winds that blow at more than 500 kilometers per hour. The image at top is a mosaic of multiple images taken through near-infrared filters. False coloring in the image reveals cloud-top heights. High, thick clouds are white and high, thin clouds are pink. Low-altitude clouds are blue. The two black- and-white images at bottom are enlargements of the boxed area; the one on the right was taken 70 minutes after the image on the left. The arrows show where clouds have formed, or dissipated, in the short interval between images. The smallest clouds are tens of kilometers across. Such dynamic systems can be monitored by autonomously operating change detection systems.

10. (right) Active volcanism is seen on Earth, Io, and Triton, a moon of Neptune. Unlike Earth and Io which exhibit high temperature silicate volcanism, the magmas on Triton are cryo-volcanic, nitrogen-rich plumes that fountain into near vacuum, before the tenuous atmosphere streak the plumes. These features have been imaged only once, by Voyager 2. What changes would have taken place when they are next seen?

14. VOLCANO: A C-Band image of Kilauea, Hawai'i. The city of Hilo can be seen at the top of the image. Also shown are the different types of lava flows around the crater Pu'u O'o. Ash deposits which erupted in 1790 from the summit of Kilauea volcano show up as dark in this image, and fine details associated with lava flows which erupted in 1919 and 1974 can be seen to the south of the summit in an area called the Ka'u Desert. In addition, the other historic lava flows created in 1881 and 1984 from Mauna Loa volcano (out of view to the left of this image) can be easily seen despite the fact that the surrounding area is covered by forest. Such information can be used to map the extent of such flows, which can pose a hazard to the subdivisions of Hilo. Mauna Loa is a decade volcano, a site of close scrutiny because of its proximity to a population center. Highway 11 is the linear feature running from Hilo to the Kilauea volcano. During these observations field teams on the ground reported that there was vigorous surface activity about 400 meters inland from the coast. A moving lava flow about 200 meters long was observed at the time of the shuttle overflight. Subsequent images taken during the October 1994 mission showed changes in the landscape due to flow emplacement. This image is centered at 19.2 degrees north latitude and 155.2 degrees west longitude (NASA PIO image P-43918).

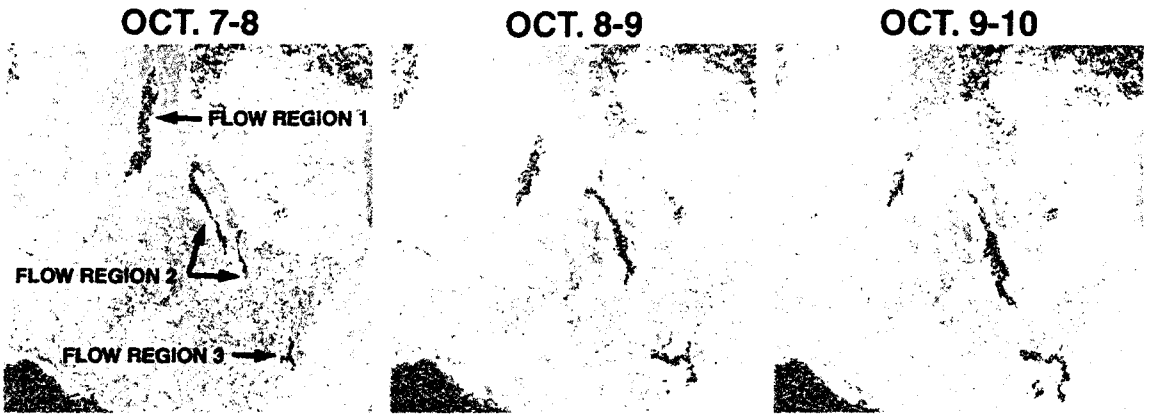

15. VOLCANO: The decorrelation of Shuttle C-SAR radar data acquired in 1994 shows the locations and areal extent of newly emplaced lava flows on the flanks of Kilauea, Hawai'I (Zebker et al., 1994). Knowing the time between observations allows average emplacement rates to be determined. Calculations were verified by ground-truth. The techniques used here can be used to make similar calculations at remote, inaccessible volcanoes, both on Earth and Io.

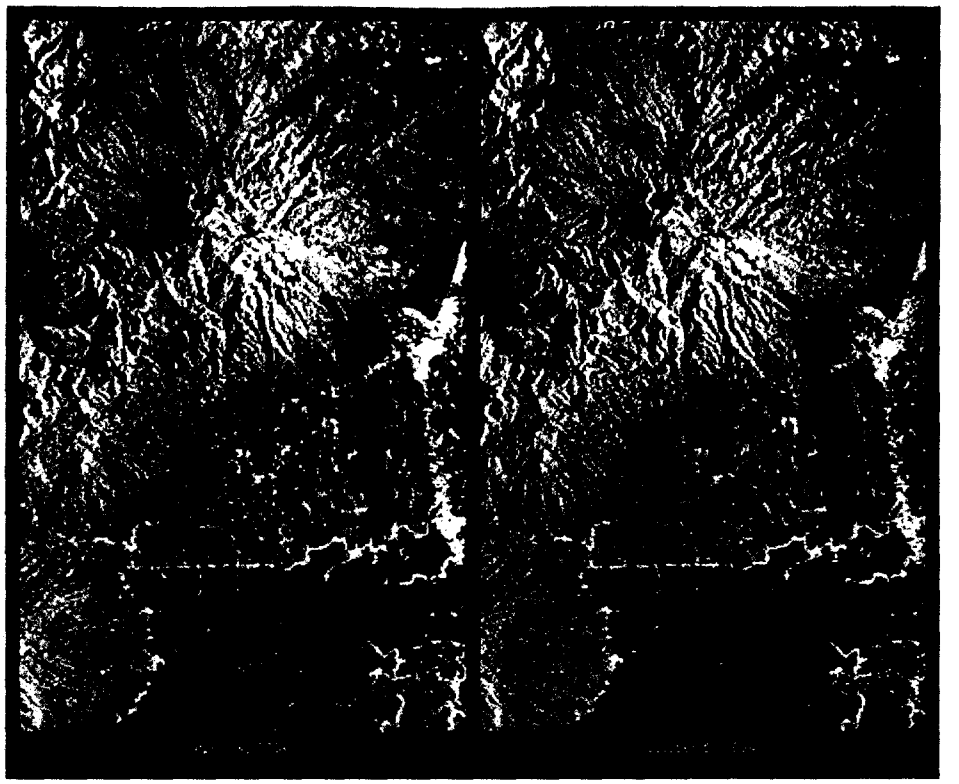

16. VOLCANO: A color composite radar images of Mt. Pinatubo, Philippines, showing lahar emplacement. These images were acquired by the SIR-C/X- SAR aboard *Endeavour* on April 14, 1994 (left image) and October 5,1994 (right image). The images are centered at about 15 degrees north latitude and 120.5 degrees east longitude. Both images were obtained with the same viewing geometry. The color composites were made by displaying the L-band (horizontally transmitted and received) in red; the L-band (horizontally transmitted and vertically received) in green; and the C-band (horizontally transmitted and vertically received) in blue. The area shown is approximately 40 kilometers by 65 kilometers (25 miles by 40 miles). The main volcanic crater on Mount Pinatubo produced by the June 1991 eruptions and the steep slopes on the upper flanks of the volcano are easily seen in these images. Red on the high slopes shows the distribution of the ash deposited during the 1991 eruption, which appears red because of the low cross-polarized radar returns at C and L bands. The dark drainages radiating away from the summit are the smooth mudflows, which even three years after the eruptions continue to flood the river valleys after heavy rain. Comparing the two images shows that significant changes have occured in the intervening five months along the Pasig-Potrero rivers (the dark area in the lower right of the images). Lahars that occured during the 1994 monsoon season filled the river valleys, allowing the lahars to spread over the surrounding countryside. Three weeks before the second image was obtained, devastating lahars more than doubled the area affected in the Pasig-Potrero rivers, which is clearly visible as the increase in dark area on the lower right of the images. Migration of deposition to the east (right) affected many communities, a total of 80,000 people. Changes in the degree of erosion in ash and pumice deposits from the 1991 eruption can also be seen in the channels that deliver the mudflow material to the Pasig-Potrero rivers. Locally, the effects of the 1991 eruption will most likely continue to impact surrounding areas for as long as the next 10 to 15 years (2001-2006). Mudflows will continue to pose severe hazards to adjacent areas. Radar observations like those obtained by SIR-C/X-SAR will play a key role in monitoring these changes because of the radar's ability to see in daylight or darkness and even in the worst weather conditions. Radar imaging will be particularly useful, for example, during the monsoon season, when the lahars form. Frequent imaging of these lahar fields will allow scientists to better predict when they are likely to begin flowing again and which communities might be at risk. {http://www.jpl.nasa.gov/radar/sircxsar/pinatubo2.html P-44729 October 7, 1994}

N 19.1/ E 19.5 Chad April 1994

N 25.5/ E 30.5 Egypt April 1994

17. AEOLIAN: Single-pass X-SAR images of barchan dunes in areas of the Sahara Desert with strong winds: a) Chad 19.1 N/ 19.5 E; b) Egypt 25.5 N/ 30.5 E. Resolution of X-SAR images prevents detection of small changes in dunes over the six-month period between the two SIR-C/X-SAR missions. Dune detection may be possible with higher ASC resolution. Each image is ~50 km across.

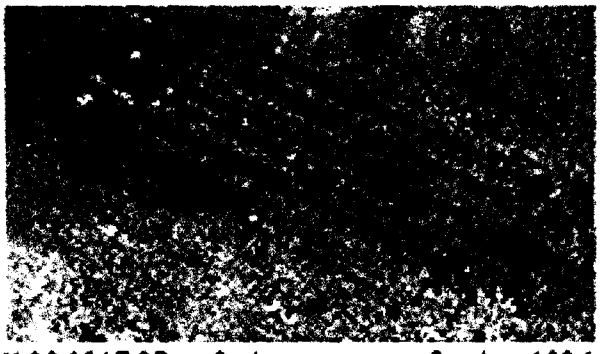

18. AEOLIAN: X-SAR images of wind streaks in a) Bolivia (18.5 S/ 68.5 W) and b) Syria (33.3 N/ 37.0 E). Images were acquired only in October 1994, so change detection is not possible. Each image is ~40 km across.

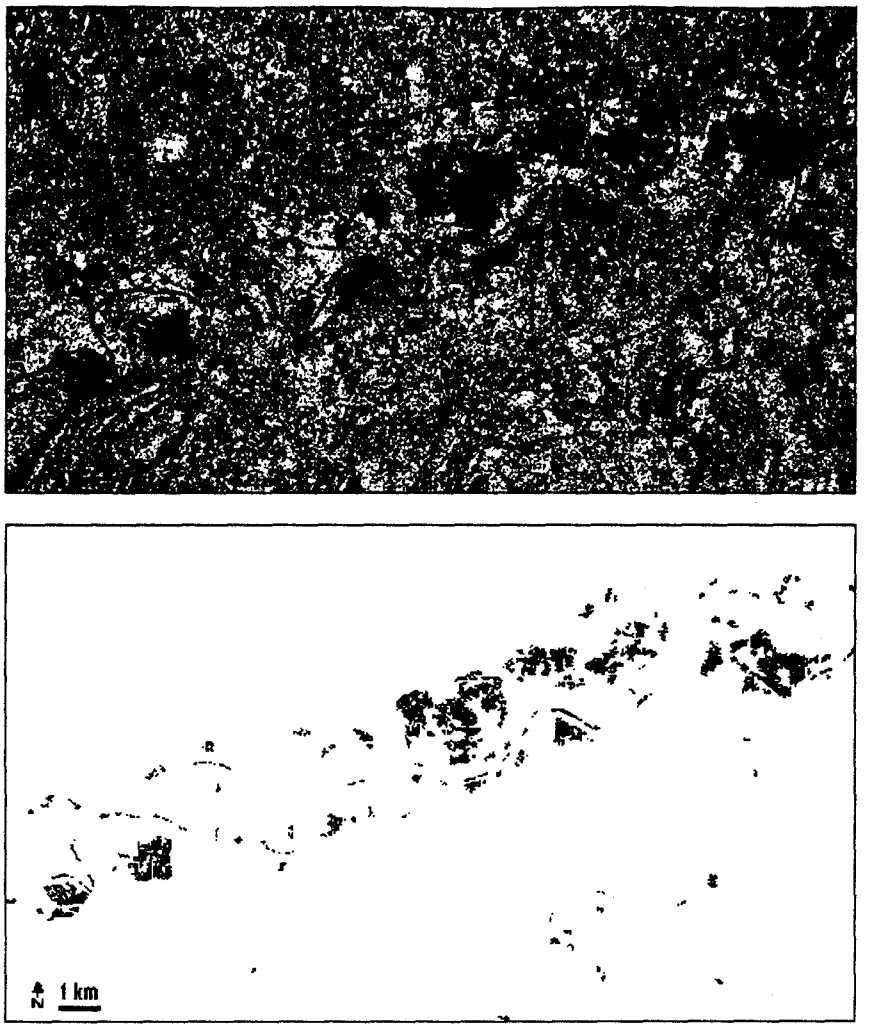

19. FLOOD: (top) flooding of the Tanaro river between Felizzano and Allessandria in 1994, as imaged by the ERS-1 SAR (Giacomelli et al. 1998). Areas of open water can be isolated based on backscatter properties (bottom image).

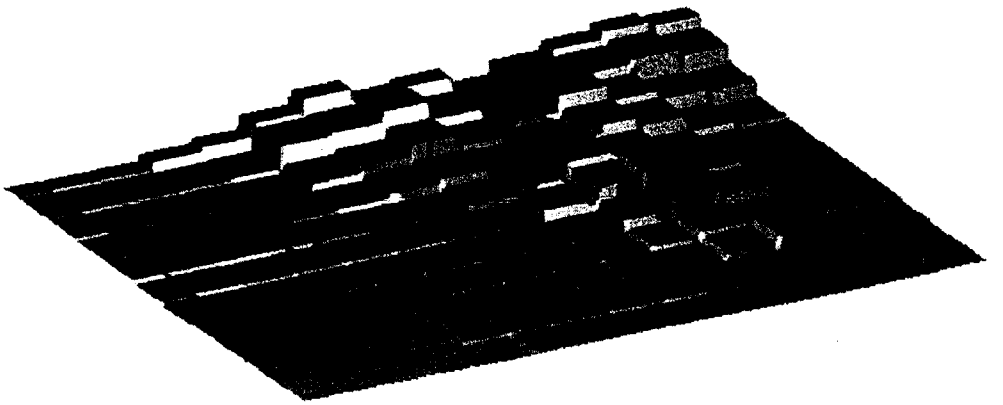

20. FLOOD: Predictions of water flow can be made by inputting the water data into Digital Elevation Models and using mathematical models of hydrological processes to predict water flow.

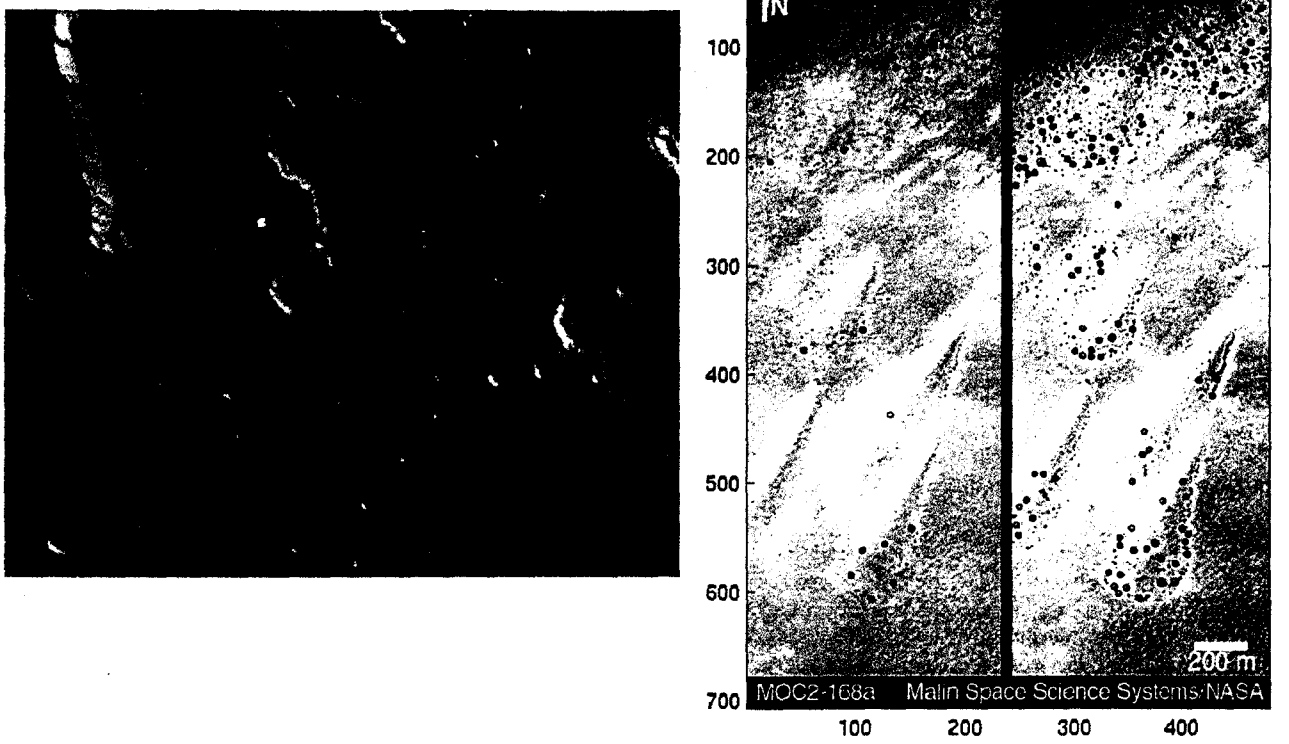

21. FEATURE ID: figure 21a (left) shows the result of a Diamond Eye run on an image of Mars, identifying impact craters (outlined in boxes). Such pattern recognition algorithms can be used to detect a wide range of features. Figure 21b (right) shows the result of a 'spot' detection algorithm on two MOC images of Mars (photos by NASA/MSSS). The new spots are easily picked out in the right-hand image. Interestingly, some spots in the left hand image have disappeared in the right hand image.

22. STATIC: The Galapagos Islands are a possible target for returning high-resolution X-SAR data for use in interferometry analyses. Over the last decades, the islands have inflated and deflated in response to pulses of magma deep beneath them. The circular volcanic craters on the islands can be used to test the Diamond Eye software.